CODE COMPARISON

This report is a summary of
"Results and Code Predictions for
ABCOVE Aerosol Code Validation
- Test AB5," HEDI-TMI 83-16.

R. K. Hilliard, Hanford Engineering
Development Laboratory

The summary was prepared by
Christopher Ryder, U.S. NRC

OBJECTIVE

This report describes the first confirmatory test in the ABCOVE program, test AB5, and compares the computer code predictions with the experimental measurements. The objective of test AB5 is to collect experimental data on aerosol behavior for use in validating aerosol behavior computer codes. The experiment is of moderate duration with a strong aerosol source generated by a sodium spray in an air atmosphere.

RELATIONSHIP TO SOURCE TERM RESEARCH

The Aerosol Behavior Code Validation and Evaluation (ABCOVE) program has been developed in accordance with the LMFBR Safety Program Plan. The ABCOVE Program is a cooperative effort between the U.S. Department of Energy, the U.S. Nuclear Regulatory Commission, and their contractors currently involved in nuclear aerosol code development, testing or application. A series of large-scale confirmatory tests are to be performed in the Containment Systems Test Facility (CSTF) vessel covering a range of aerosol source release rates, source duration times, and aerosol composition. When experiments cannot be performed under the full range of postulated accident conditions the experiments must demonstrate that all of the significant aerosol mechanisms have been properly modeled and that the assumptions used in the modeling are valid.

EXPERIMENTAL FACILITY AND INSTRUMENTATION

The test was performed in the Containment Systems Test Facility (CSTF). The CSTF is a model containment vessel which is located in a ventilated concrete building. Associated equipment includes a sodium supply system, instrumentation system, control room and data acquisition system, data reduction and analysis system, chemical laboratory rooms, utility services, maintenance shop, and offices.

Containment Vessel. The CSTF containment vessel is a 850-m^3 (30,000-ft^3) carbon steel vessel with a design pressure of 0.517 MPa gauge (75 psig). All interior surfaces are coated with a modified phenolic paint, and exterior surfaces are covered with a 25.4-mm layer of fiberglass insulation with an outer aluminum vapor barrier.

Sodium Spray System. Commercial grade sodium is melted in a portable clam shell heater and charged into the sodium supply tank. The supply tank is suspended from a lead cell so that the combined weight of tank and sodium can be measured. Two valves and a magnetic flowmeter are located in the sodium line. Two sodium spray nozzles are installed in the containment vessel 4.2 m above the catch pan. The nozzles are hollow cone types oriented to spray in the upward direction.

Aerosol Characterization. The suspended mass concentration, the particle size distribution, and the chemical composition is measured periodically by direct sampling at various times and locations during the tests. In addition, some information on shape and size is obtained by electron microscopy.

The mass concentration of suspended particles is measured as a function of time by periodically passing a measured quantity of gas through small filters located directly in the containment atmosphere and subsequently analyzing the material collected on the filter for total mass and for Na. Two types of sampling techniques are used: in-vessel fiter clusters and through-the-wall samplers.

The aerodynamic size distribution is determined by sampling with cascade impactors inserted through the wall. Two types of cascade impactors are used: Andersen Mark III 8-stage and Sierra model 225 6-stage. Previous tests have shown that these instruments give good agreement when properly calibrated. Glass fiber collection surfaces provided by the manufacturers are used.

Chemical identification of the aerosol is determined at various times during each test by collecting aerosol on a membrane filter paper at a wall station and analyzing for various chemical species by x-ray diffraction and wet chemistry. The sample is protected from ambient atmosphere to minimize chemical changes that might occur after the sample is taken.

The instantaneous deposition rate of particles is measured by exposing coupons in a horizontal orientation for brief periods. The top surface of the coupon is washed and the rinse water analyzed for sodium. The deposition rate is calculated as a total mass flux of particles. No information is obtained on settling as a function of particle size by this technique. The "deposition velocity" was calculated by dividing the flux by the airborne concentration.

Temperature Measurement. All temperatures are measured by calibrated Chromel-Alumel thermocouples with stainless steel sheaths. Readout is in parallel on strip chart recorders, magnetic tape, and paper tape.

Pressure Measurement. The absolute pressure and the gauge pressure in the containment vessel is measured by a pressure transducer and a Heise gauge. The differential pressure between the cover gas in the sodium supply tank and the containment atmosphere is measured by a differential pressure transducer.

Gas Analysis System. The composition of the containment gas is measured continously at five locations by pulling samples through tubing to on-line analyzers located ex-vessel. Filters at the tube inlet prevent aerosol from entering the analyzers. A few grab samples are taken for subsequent analysis by mass spectrometry.

Data Acquisition System. Many of the key experimental measurements are made manually and periodically, such as the filter samples, the cascade impactor-samples, the electron microschop samples, and the chemical analysis. The data associated with these manual samples are logged by technicians onto data sheets or recorded in notebooks.

The on-line instrumentation includes thermocouples, pressure transducers, a sodium flowrate mater, a sodium supply tank load cell, and gas analyzers for O_2, H_2 and water vapor. The output of these sensors is recorded in parallel on strip chart recorders and on a 120-channel digital data acquisition system. For test AB5, 108 channels are recorded on magnitic tape every 9.0 seconds initially, with decreasing frequency at later times. For times greater than 90 minutes, the measured parameters change more slowly.

Chemical Analyses. Filter papers from cascade impactors, through-the-wall aerosol concentration samplers, and in-vessel fiter clusters are analyzed for sodium by either acid titration or emission spectrometry. Corrections are made to account for background sodium in the filter paper and demineralized water. Approximately half of the fiter papers are weighed before and after exposure to determine the total mass of aerosol on the paper. Chemical forms of aerosol are determined by performing a combination of chemical techniques, including x-ray diffraction, chromatography, and wet chemistry for metallic Na, Na_2O_2 and CO_2 content.

RESULTS

Particle Size Measurement. The data from the cascade impactor, the electron microscope photographs, and the deposition coupons are compared. The output of the cascade impactor measurements is the AMMD. The settling mean diameter, d_s, is the output of the deposition coupon and mass balance computations. In order to compare the three methods, the cascade impactor data are converted to settling mean diameters. If the particle size distribution is log-normal, the aerodynamic settling mean diameter can be calculated from the cascade impactor data;

$$d_s = \text{AMMD} \exp(\ln^2 O_g)$$

where: d_s = aerodynamic settling mean diameter

O_g = geometric standard deviation

The ratios of d_s measured by the various methods averaged near unity for the entire test period, hence, the methods are in general agreement. However, a significant discrepancy is noted between the cascade impactor measurement and the mass balance method for the time period bracketing the source cutoff; the impactor method showed that the particle size increased to very large values immediately after source cutoff; the size calculated by mass balance on the containment atmosphere showed that the particle size decreased steadily after source cutoff. One explanation is that the impactor data for the time immediately after source cutoff are based on one sample (T316) in which 53% of the aerosol mass is greater than the first stage cutoff diameter. Thus, no information is available concerning the distribution of particles larger than 20 um.

The assumption of log-normality may be inapplicable on this sample. The deposition coupon data agree well with the other methods except for the samples taken at longer times when the suspended concentration is low. Small quantities of resuspended aerosol might have contaminated the coupons and biased the measurement toward larger sizes.

Eleven individual code cases are run both prior to the test and after the test. The post-test runs are done "blind" in that no experimental data on aerosol behavior is made available; only information on the thermal conditions and aerosol mass is made available. Pretest predictions are based on a test plan and chosen inputs. After the AB5 test is completed, data are transmitted to the participants.

Most of the code cases used identical or very similar numerical values. The exception is the source size for the MAEROS code. The MAEROS uses discretized distributions and, for the post-test case, all of the particles are placed in the bin whose diameter limits ranged from 0.1809 um to 0.2599 um. The use of the one size bin simplified the setup of the code case. The difference in source size do not have a great impact on predicted aerosol behavior. Because of differences in modelling, the same input parameters for different codes may not infer the same calculations.

Some input parameters are as follows:

CHI is a dynamic shape factor that allows the particle drag to be related to Stokes' law for spheres. CHI is a denominator factor in Stokes' law. Because non-spherical agglomerates settle more slowly than sperical agglomerates, CHI is equal to or larger than unity.

GAMMA is a factor which relates the effective collision radius of a particle to the actual particle radius. Because non-spherical agglomerates are able to collide more effectively than spherical agglomerates, GAMMA is equal to or larger than unity.

ALPHA is a density modification factor used to account for the reduced settling velocity of agglomerates compared to solid spheres. Generally, it is a numerator factor in Stokes' law and its value is less than or equal to unity.

EPSILON is a gravitational collision efficiency used in the HAA codes. It relates to the fraction of particles in a swept volume that is captured by a falling particle.

KLYACHKO is a parameter that allows deviations from Stokes' drag to occur at high Reynolds numbers to be taken into account. This factor becomes important for particles larger than 100 um.

The valuse of most parameters are selected by comparing code predictions with earlier large-scale sodium fire aerosol tests in the CSTF. The selected variables cover a significant numerical range. Diffusional plating boundary layer thickness is assigned values from 1×10^{-4} m to 1.5×10^{-7} m, a variation of three orders of magnitude. The small value for delta used in the HAA-3 code results from the assumption that all plateout is caused by diffusion; delta is assigned an empirical value to match previous experiments. The wall temperature gradient values range from 4.7×10^{2} °K/m to 1.6×10^{5} °K/m, almost three orders of magnitude. The assigned values of the ratio of gas to particle thermal conductivity varies from 0.001 to 0.11, two orders of magnitude.

COMPARISON WITH THEORY AND CODES

Some predicted parameters of the aerosol behavior are compared with each other and with the experimenal data.

Suspended Mass Concentration. The concentration predicted by log-normal codes decreases more rapidly than the data after the end of the source period. The discrete codes give good agreement with experiment after the end of source period. All codes agreed with the data within a factor of 2 for the high concentration period.

Aerodynamic Mass Median Diameter (AMMD). The log-normal codes generally overpredict the AMMD. The discrete codes underpredict the AMMD. For the first few hundred seconds, all codes underpredict the AMMD, which suggests that the code input values for source particle size are too small.

For the MAEROS code, the AMMD is not reported. The values for MAEROS are calculated by plotting the size distribution on log-probability paper. The mass median diameter (MMD) obtained from this plot is converted to AMMD;

$$AMMD = MMD \left(\frac{p}{x}\right)^{1/2}$$

where: p = material density of aerosol particle
x = dynamic shape factor

The data obtained from measurements using cascade impactors. Since the impactor measurements are not made precisely at the computer code times, the measured values are extrapolated experimental AMMD as a function of time.

A factor of 1.5 is used for evaluating particle size parameters rather than a factor of two as is done for other parameters. Particle sizes and standard deviations do not vary over as wide a range as other parameters and, for this reason, the error band is assigned a value of 1.5.

Geometric Standard Deviation (σ_g). Compared with cascade impactor data, the log-normal codes underpredict σ_g. The discrete codes are generally better, but overpredict σ_g during the source release period and underpredict σ_g after the source ended.[9] Values for σ_g are not reported for the MAEROS and CONTAIN codes; the values for MAEROS and CONTAIN are calculated by plotting the reported size distributions on log-probability paper and using the equation below to determine an approximate value for σ_g;

$$\sigma_g = \frac{84.1\% \text{ size}}{50\% \text{ size}}$$

Although this method is not rigorous for size distributions that are not log-normal, it is believed to be reasonable.

The experimental measurements are not made at precisely the times reported for the computer codes, the measured values for σ_g are plotted and the data are taken from this curve for the desired times.

The number of times that individual code cases predict the experimental value within a factor of 1.5 is determined. The comparisons may not be relevant for the discrete codes because the distribution is not usually log-normal and a well-defined σ_g may not exist.

Aerodynamic Settling Mean Diameter (d_{sa}). The aerodynamic settling mean diameter, d_{sa}, is defined as the diameter of a unit density spherical particle which has a settling velocity equal to the sedimentation velocity for the whole aerosol. The experimental data are calculated from the rate of change of suspended mass concentration, a knowledge of the source release rate, and Stokes' law for settling of unit density spheres. Wall plating is insignificant compared with sedimentation.

All of the codes are generally able to predict the d_{sa} better than the AMMD. The codes which underpredict the AMMD also overperdict the σ_g and vice versa. Since the settling mean diameter is proportional to both AMMD and σ_g, the errors in predicting AMMD and σ_g tend to compensate and result in a reasonably good prediction of d_{sa}. The number of times that individual code cases predicted the experimental value with a factor of 1.5 is determined.

Leaked Mass. An estimate of leaked mass is not provided by the MAEROS code; the experimental values from which its curve is drawn are calculated assuming the aerosol leak is at a constant rate of 1% per day of the suspended mass.

The codes are generally more accurate in predicting leaked mass than they are in predicting suspended mass concentration at discrete times. The number of times that individual code cases predict within a factor of two the experimental value is determined.

Settled Mass. The settled mass is measured experimentally only at the end of the experiment. All of the codes accurately predict the settled mass with nine of the 11 cases predicting within 10% of the test result. Since all the codes show that settling is complete by 10^4 seconds, the end-of-the test result is reported for times 10^4 and later.

The number of times that individual code cases predict the experimental value within $\pm$15% is determined.

Plated Mass. The plated mass is measured at the end of the test. The code predictions range from 1.7% to 1000% of the measured value. Four of the code cases predict the experimental value within a factor of two. The code predictions for plated mass have the most variability in accuracy than for any other parameter except suspended mass concentration.

SUMMARY

The codes in the ABCOVE program which use the log-normal assumption are HAA-3, HAA-4, and HAARM-3. The codes which use the discrete particle size groups are QUICK, MSPEC, MAEROS and CONTAIN. Each type of code has its advantages and disadvantages. Discrete codes are usually more accurate than log-normal codes, but log-normal codes are usually more efficient. No comparison of efficiencies is attempted for test AB5.

Test AB5 uses a high sodium spray rate for a sufficiently long time so that high aerosol concentrations are achieved. Agglomeration is important. Previous studies carried out by the ABCOVE participant from Battelle Columbus indicate that the log-normal assumption causes an overestimate of agglomeration. The high aerosol source rate used in test AB5 is chosen to explore this apparent limitation of log-normal codes.

A comparison between any two codes is difficult without considering differences in input parameters. Comparing average values of parameters is inadequate, but this is done for suspended concentration and particle size parameters.

The following tendencies for suspended concentration are evident:

- Discrete codes tend to predict close agreement or low during the source release period compared to data. The concentration decreases at a slightly lower rate than data after source termination.

- Log-normal codes tended to predict high during the source period and to give a more rapid concentration decrease after the source termination compared with data.

- o The log-normal codes tend to overpredict the AMMD at all times and underpredict the σ_g for all except the latter stages of the source release period, compared with data.

- o The discrete codes tend to underpredict the AMMD at all times and overpredict σ_g during the source period, compared with data.

- o Both discrete codes and log-normal codes predict the aerodynamic settling mean diameter reasonabley well during the source period compared with data. The discrete codes predict best after the source is terminated. .

The discrete codes appear to predict aerosol behavior both during the source period and after source termination better than log-normal codes. The discrete codes compare more favorably with the data if plateout had not been overpredicted by two cases involving discrete codes. The overpredicted plateout causes an underpredicted concentration during the source period and a slow decrease in concentration after source termination. While the more rapid concentration decay predicted by the log-normal codes does not significantly affect the leaked mass calculation (at constant leak rate), it could be important for accident cases where a containment fail after source termination. For example, at 30,000 sec. (8.3 hr.), the mean of the log-normal codes underpredict the concentration by a factor of 22. However, the concentration at 30,000 sec. is only 0.0004 that of the maximum value during the source period.

Brownian diffusion and thermophoresis is used to model plateout. For the HAA-3 codes, thermophoresis is not included as a deposition mechanism; diffusion is the only plateout mechanism for these two codes. Predicted values of plated mass vary by several orders of magnitude. Predicted values of plated mass vary from 3.17×10^{-2} g (QUICK, ORNL) to 1.9×10^{3} g (MAPEC, BCL). Part of the discrepancy between the two extremes is due to differences in input values for the thermal gradient. The input values for peak gradients vary by a factor of 10 between the two codes. This difference in gradients is expected to cause as much as an order of magnitude difference, but not an observed difference of a factor of 600. It is apparent that other differences must also exist. Of interest is the difference in predictions when the same inputs are used; HAARM-3 predicts a plated mass of 2.2×10^{4} g, QUICK and MSPEC predicts plated masses, 8 times larger.

Some deviations from the test plan occur and require blind post-test predictions to be made. A significant change from the test plan is the aerosol source rate, which is 0.770 of the test plan value. Other deviations include: the sodium fraction in the aerosol is 0.574 rather than 0.588; the material density is 2.50 rather than 2.72; and the containment temperature and pressure are slightly lower than planned. The total mass of aerosol released is 0.746 of the test plan value.

Some of the variation arises because the codes do not predict for the entire 4×10^5 second period; thus the number of codes being averaged change with time (after 10^4 sec.). The post-test predictions for suspended concentration, leaked mass, settled mass and plated mass averaged 70% of the pretest values. Pretest predictions might seem to be unnecessary as long as blind post-test predictions are needed. The merit of performing the analyses prior to experiment is that no beneficial knowledge of test results are available when the predictions are made.

FUTURE PLANS

The three experiments have been completed. Test AB5 is described in this summary. Test AB6 is done on an aerosol system made of two chemical species. Test AB7 is done to address issues arising from test AB6.

Several chemical analyses have yet to be completed. The results will be reported.

Enclosure

INDEX

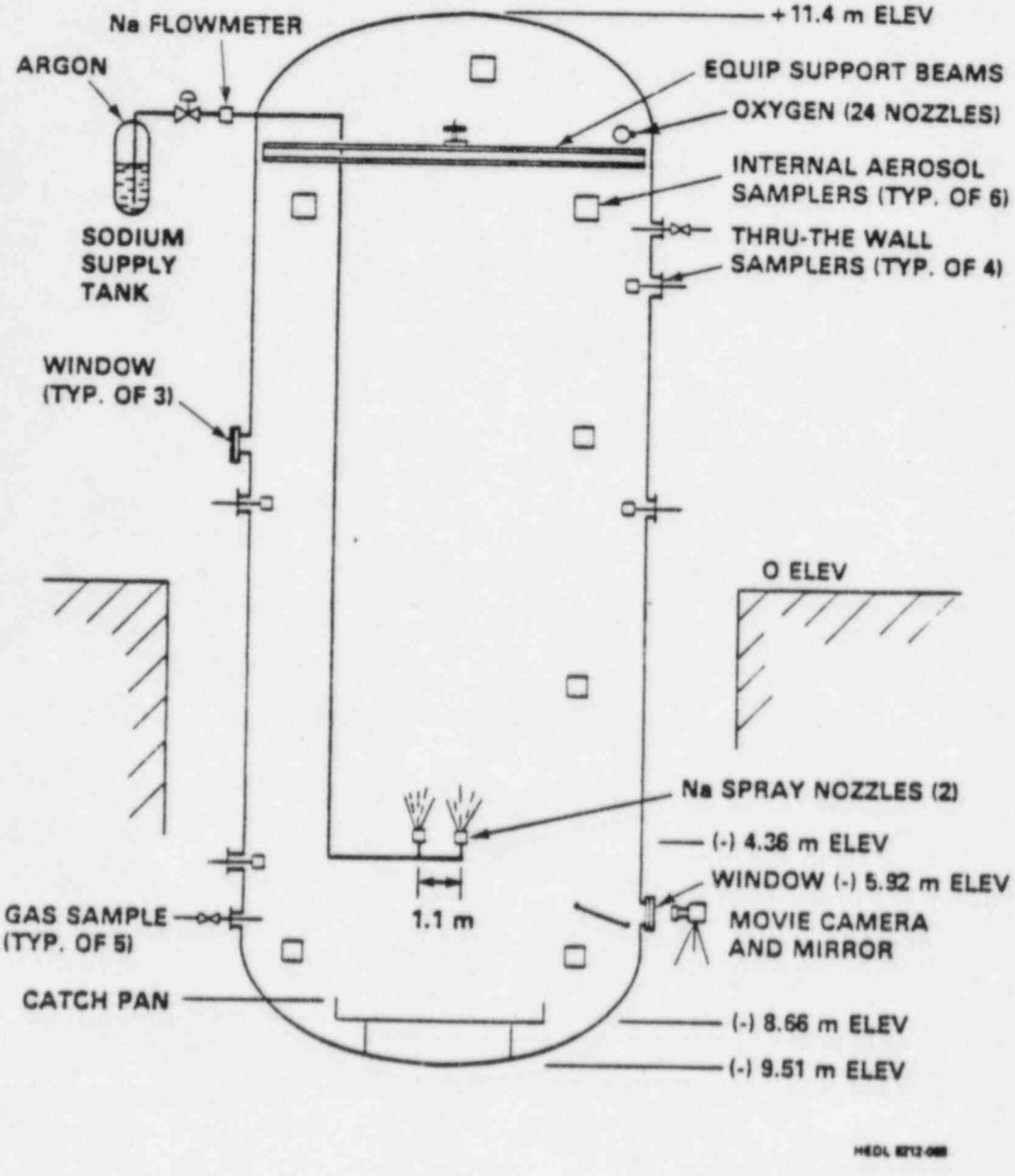

Schematic Elevation View of the CSTF Containment Vessel Arrangement for Test AB5.

CSTF CONTAINMENT VESSEL PROPERTIES

General

Code	ASME Section VIII, 1962
Material	Carbon Steel, SA 212-B
Interior paint (phenolic)	0.51 mm
Exterior thermal insulation	Fiberglass, 25 mm thick, k = 0.0467 W/m°C @ 100°C
Design pressure	0.517 MPa at 160°C (75 psig at 320°F)
Nominal leak rate	1.0% per day

Dimensions

Diameter (ID)	7.62 m
Overall height	20.3 m
Cylinder height	16.5 m
Enclosed volume	852 m^3

Weight, kg (lb)

Top head	8,753
Bottom head	8,753
Cylinder	69,390
Penetrations and doubler plates	10,295
Catch pan	500
Internal components	5,580
Total Weight	103,260

Surface Areas for Heat Transfer, m^2

Top head	63.0
Bottom head	63.0
Cylinder	394
Total area for heat transfer to environs	520
Internal components	232

Surface Areas for Aerosol Settling, m^2

Bottom head	36.7
Catch pan	11.1
Personnel deck	4.2
Internal components	36.2
Total	88.3

Surface Areas for Aerosol Plating, m^2

Vessel shell	520
Internal components	232
Total	752

Thickness for Heat Transfer, mm

(Average lumped values)*	
Top head	18.1
Bottom head	18.1
Cylinder	22.9
Internal components	3.4

*Average Thickness = $\frac{\text{Weight}}{\text{rea) (density of steel)}}$

SODIUM SPRAY SYSTEM CHARACTERISTICS

Number of nozzles	2
Nozzle orientation	upward
Sodium temperature	563°C
Pressure drop across nozzle	200 kPa (29 psi)
Sodium spray rate	265 g/s
Nozzle distance above catch pan	4.2 m
Nozzle orifice diameter	5.51 mm
Spray angle	72°

SUMMARY OF TEST CONDITIONS FOR TEST AB5

Test Condition	Value
Initial Containment Atmosphere	
Oxygen concentration	23.3 ± 0.2 vol %
Temperature, mean	29.1°C
Pressure	0.122 kPa (17.7 psia)
Dew point	16 ± 2°C
Nominal leak rate	1% per day at 10 psig
Sodium Spray	
Sodium spray rate	256 ± 15 g/s
Spray start time	13 s
Spray stop time	885 s
Total Na sprayed	223 ± 11 kg
Sodium temperature	563°C
Spray drop size, MMD	1030 ± 50 μm
Spray size geom. std. dev.	1.4
Oxygen Concentration	
Initial O_2 concentration	23.3 ± 0.2 vol %
Final O_2 concentration	19.4 ± 0.2 vol %
Oxygen injection start	t = 1 minute
Oxygen injection stop	t = 14 minutes
Total O_2 injected	47.6 std. m^3
Containment Conditions During Test	
Maximum average atmosphere temperature	279°C
Maximum average temperature of steel vessel	93.5°C
Maximum pressure (absolute)	213.9 kPa (31.0 psia)
Final dew point	-1.5°C (29°F)
Aerosol Generation	
Generation rate, g/s as aerosol	445
Mass ratio, total to Na	1.74
Material density, g/cm^3	2.50
Initial suspended concentration	0

SODIUM MASS BALANCE

	m^2	kg Na	kg Na/m^2
Delivered to Containment[a]		222.8	
Recovered from Containment[b]			
Bottom Head	36.7	117.2	3.19
Catch Pan	11.2	42.8	3.81
Personnel Platform	4.2	15.4	3.68
All other Surfaces[c]		67.4	
Total CV Washes		242.8	
Samples		2.2	
Total Accounted For		245.0	
Difference		22.2 gain	

(a) Measured by load cell on Na supply tank.
(b) Measured by water wash volume and Na concentration.
(c) Vertical walls, top dome and internal components.

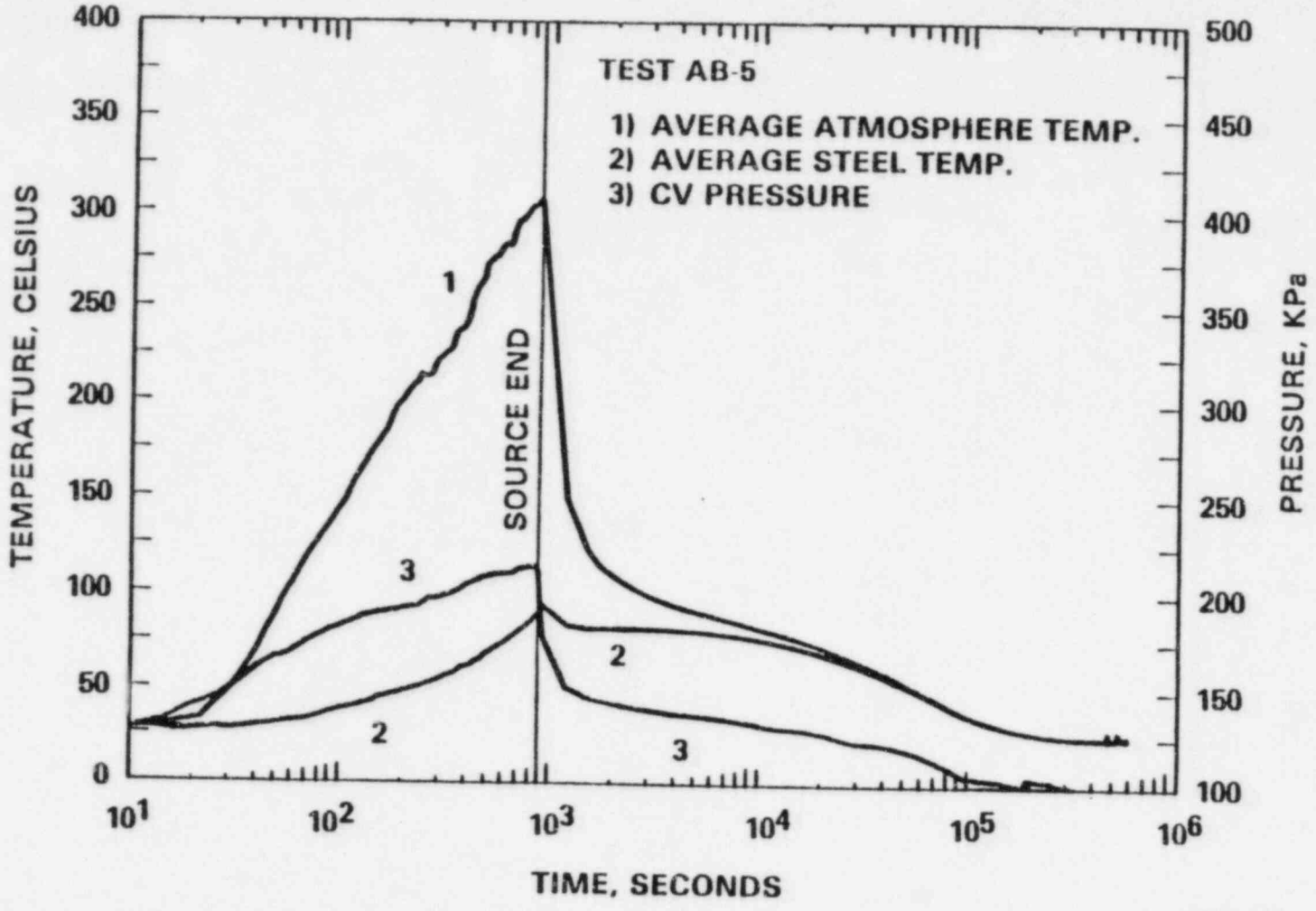

Containment Temperature and Pressure as a Function of Time.

SUMMARY OF INFORMATION ON
AEROSOL SOURCE PARTICLE SIZE

	Method	MMD (μm)	σ_g
1.	Electron microscope sample at 1140 s. Optical sizing.	$0.63^{+0.55}_{-0.27}$	2.25 ± 0.25
2.	Cascade impactor sample taken at 63 s.	1.6 ± 0.07	1.9 ± 0.2
3.	Test plan assumed, based on literature.	0.5	1.5

COMPARISON OF AEROSOL SIZE IN CONTAINMENT ATMOSPHERE AS MEASURED BY VARIOUS METHODS

Time (s)	d_s, Settling Mean Diam. (um)			Ratio of d_s Measured		
	Cascade Impactor(a)	Dep. Coupon(b)	Mass Balance(c)	Coupon To Imp.	Mass Bal. To Imp.	Mass. Ba.. To Coupon
3.00 (2)(d)	37.1		25.0		0.67	
4.00 (2)	24.3		60.5		2.49	
5.00 (2)	19.4		49.6		2.55	
8.85 (2)	18.4		49.6		2.55	
1.00 (3)	66.2		46.1		0.70	
1.26 (3)	129.		33.8		0.26	
2.08 (3)	33.8	20.9(e)	20.7	0.62	0.61	0.99
3.18 (3)	23.8	18.9	14.5	0.79	0.61	0.77
5.30 (3)	14.6	16.3(e)	11.3	1.12	0.77	0.69
7.50 (3)	9.84		9.04		0.92	
1.07 (4)	8.32	10.2	7.82	1.22	0.94	0.77
1.62 (4)	6.98	10.9(e)	6.45	1.56	0.92	0.59
3.50 (4)	5.07	8.5(e)	4.39	1.68	0.87	0.52
5.00 (4)	4.65		3.77		0.81	
1.00 (5)	3.65		2.69		0.74	
2.05 (5)	2.88		1.98		0.69	
Mean				1.17	1.07	0.72

(a) Calculated by Equation (11) using Figures 21 and 22.
(b) From Table 18.
(c) From Table 19.
(d) Numbers in parenthesis are exponents of ten.
(e) Average of multiple measurements.

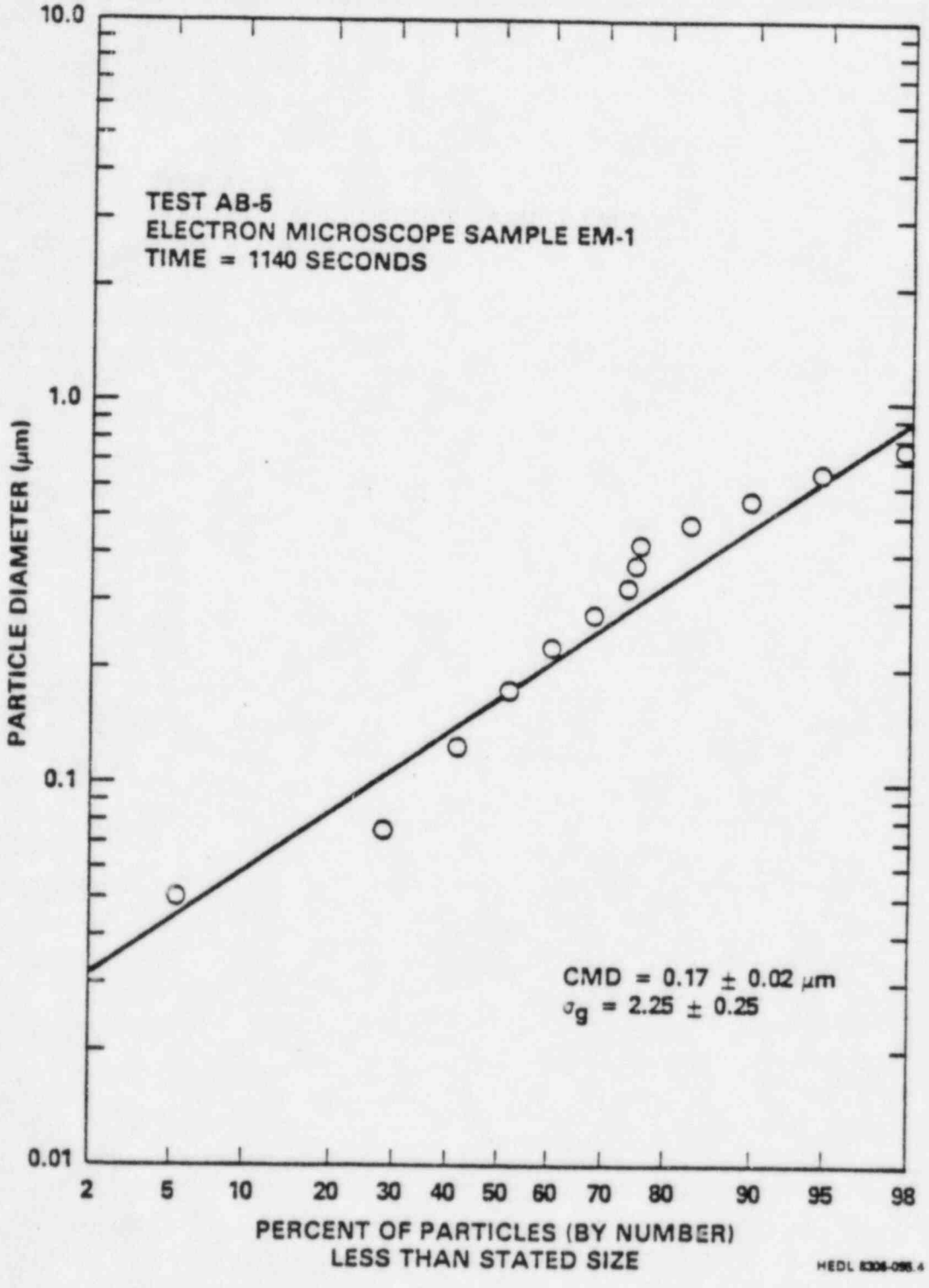

Log-Probability Plot of Primary Particle Size Distribution.

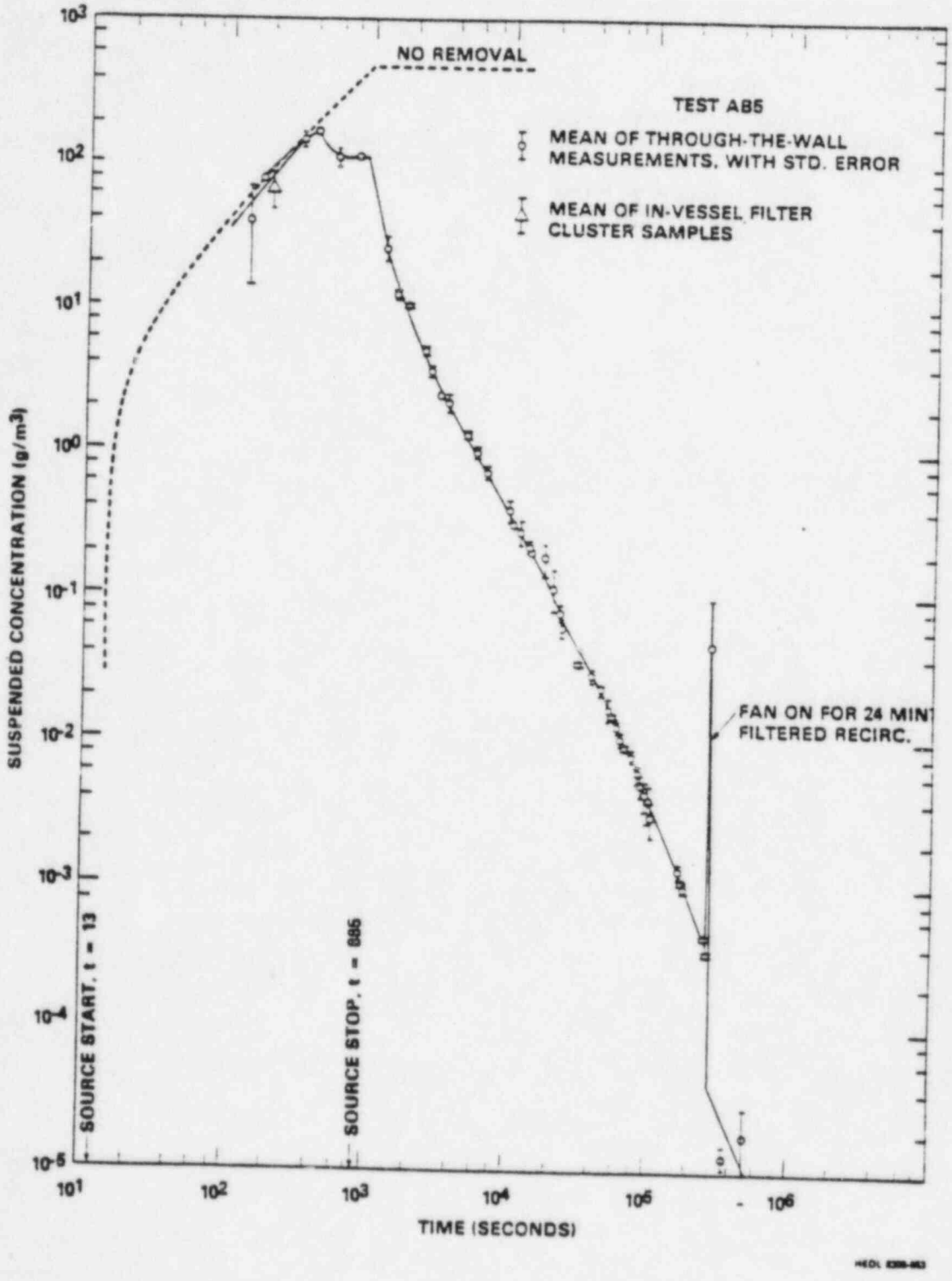

Suspended Mass Concentration in the Containment Atmosphere.

MASS SPECTROMETRIC ANALYSES OF GRAB SAMPLES
FROM CONTAINMENT ATMOSPHERE

	Vol % on Dry Basis at Specified Time and Location							
	-45 min	17 min		120 min		1440 min		
Gas	+6.1 m	+6.1 m	-6.7 m	+6.1 m	-6.7 m	+6.1 m	-6.7 m	-4.9 m
O_2	22.7	18.3	20.7	19.3	19.4	19.3	19.7	19.4
H_2	<0.01	<0.01	<0.01	<0.01	<0.01	<0.01	<0.01	<0.01
N_2	76.3	80.6	78.3	79.7	79.5	79.6	79.2	79.6
CO_2	0.09	0.05	0.07	0.06	0.07	0.06	0.07	0.07
A	0.93	1.00	0.97	0.99	0.99	1.00	1.00	1.00
CH_4	<0.01	<0.01	<0.01	<0.01	<0.01	<0.01	<0.01	<0.01
CO	<0.5	<0.5	<0.5	<0.5	<0.5	<0.5	<0.5	<0.5

EXPERIMENTAL MEASUREMENTS AND ACCURACY

Measurement	No. of Locations	No. of Times	Standard Error	Method
Suspended aerosol mass concentration	6	1	± 25%	In-vessel filter clusters
Suspended aerosol mass concentration	4	52	± 15%	Through-the-wall samplers
Aerosol particle size and σ_g	3	16	± 20%	Cascade impactor
Aerosol particle size (actual)	1	2	N/A	Electron microscopy, sizing
Aerosol particle shape	1	2	N/A	Electron microscopy
Aerosol chemical composition	1	5	N/A	Various; Chemistry Lab.
Aerosol instantaneous deposition rate	1	9	± 20%	Through-the-wall coupons
Integral settled mass/unit area	23	1	± 10%	Fall-out pans
Integral plated Na on vessel walls per unit area	7	1	± 20%	Vessel wall smears
Aerosol settled/unit area during Na spray period	1	2	± 25%	Special samplers
Na mass deposited in catch pan	1	1	± 10%	Wash and analyze for Na
Total settled Na mass	1	1	± 10%	Wash vessel floor
Total Na wall plateout	1	1	± 30%	Wash vessel walls
Temperature of containment atmosphere	28	(a)	± 2%	Thermocouples
Temperature of vessel surface	18	(a)	± 2%	Thermocouples
Temperature of Na sprayed	2	(a)	± 2%	Thermocouples
Containment pressure	1	(a)	± 1%	Pressure Transducer
Containment O_2 concentration	5	(a)	± 2%	On-line O_2 analyzer
Containment H_2 concentrations	5	(a)	± 20%	On-line H_2 analyzer
Containment moisture concentration	2	(a)	± 30%	On-line humidity analyzer
Convection velocity	1	5	Unknown	Anemometer
Sodium Spray mass flow rate	1	(a)	± 10%	Magnetic flowmeter and load cell
Overall Na mass balance	N/A	1	± 10%	Weighing, washing, volume, chem. analysis, calculation

(a) Continuous

LIST OF PARTICIPANTS FOR ABCOVE TEST AB5

Participant	Affiliation	Address
Emil Gluekler	General Electric Company	P.O. Box 5020 310 DeGuigne Drive Sunnyvale, CA 94086
R. K. Hilliard	Hanford Engineering Development Laboratory Safety Systems Development	P.O. Box 1970 Richland, WA 99352
Hans Jordan	Battelle Columbus Laboratories	505 King Avenue Columbus, OH 43201
T. S. Kress	Oak Ridge National Laboratory	P.O. Box X Oak Ridge, TN 37830
K. K. Murata	Sandia National Laboratories	P.O. Box 5800 Albuquerque, NM 87115
J. M. Otter	Rockwell International Energy Systems Group	8900 De Soto Avenue Canoga Park, CA 91304
M. G. Piepho	Hanford Engineering Development Laboratory Containment Systems Analysis	P.O. Box 1970 Richland, WA 99352

CODE CASES FOR TEST AB5

Code Case No.	Code	User
1	HAA-3B	GE
2	HAA-3C	HEDL/SSD
3	HAA-4	ROCKWELL/ESG
4	HAARM-3	HEDL/SSD
5	HAARM-3	BCL
6	HAARM-3	ORNL
7	QUICK	BCL
8	QUICK	ORNL
9	MSPEC	BCL
10	MAEROS	HEDL/CSA
11	CONTAIN	SNL

PRETEST INPUT PARAMETERS TRANSMITTED TO
CODE USERS BY THE TEST PERFORMER

Parameter	Value
Source rate, g/s cm^3	6.8×10^{-7}
Source 50% radius, μm	0.25
Source sigma, σ_g	1.5
Initial aerosol concentration	0
Source cutoff time, sec.	900
Maximum time, days	5
Leakage rate, %/day	1.0 (constant)
Settling area, cm^2	8.8×10^5
Plating area, cm^2	7.5×10^6
Volume, cm^3	8.5×10^8
Density of aerosol, g/cm^3	2.72
Temperature of atmosphere	Figure 26
Temperature of CV walls	Figure 26
Pressure	Figure 26

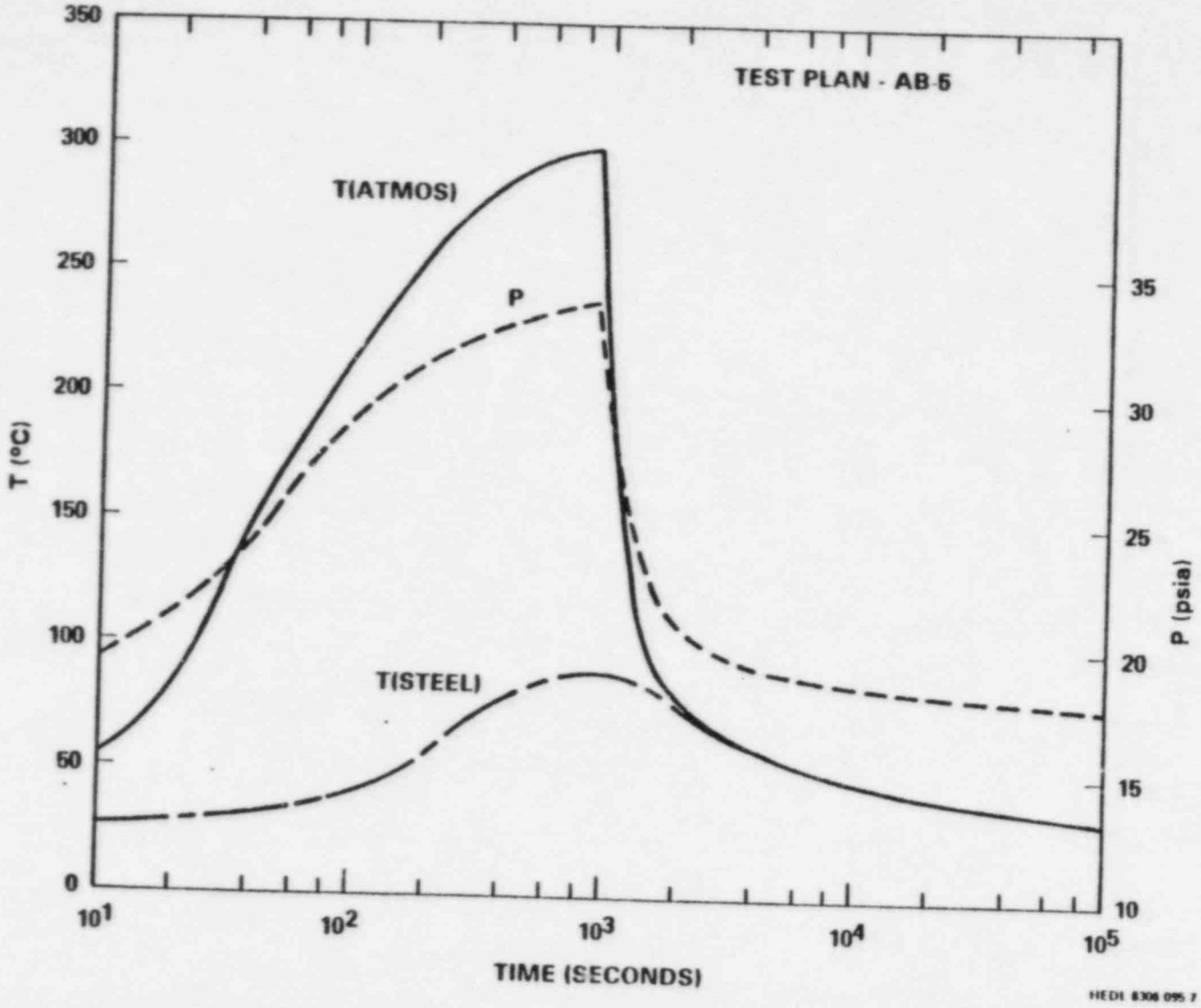

Pretest Estimates of Temperature and Pressure Provided by the Test Performer.

TEST CONDITIONS TRANSMITTED TO CODE USERS
FOR USE IN MAKING BLIND POST-TEST PREDICTIONS

Parameter	Pretest Test Plan	Post-Test Measured or Estimated
Pressure Drop Across Spray Nozzle (psi)	40	29
Sodium Spray		
Sodium Spray Rate (g/s)	340	256
Spray Start Time (s)	0	13
Spray Stop Time (s)	900	885
Total Na Sprayed (kg)	306	223
Sodium Temperature (°C)	560	563
Spray Drop Size, MMD (μm)	980	1030
Spray Size Std. Dev. (σ_g)	1.4	1.4
Aerosol Generation		
Mass Ratio, Total to Na	1.70	1.74
Generation Rate (g/s)	578	445
Material Density (g/cm^3)	2.72	2.50
Initial Time (s)	0	13
Cutoff Time (s)	900	885
Initial Conc.	0	0
Source Mass Median Radius (μm)	0.25	0.25
Source Sigma	1.5	1.5

CODE INPUT PARAMETERS RELATED TO THE AEROSOL SOURCE

Code	User	Material Density (g/cm^3)	Source Size		Source Rate	
			d_{50} (μm)	σ_g	(No./s cm^3)	(g/s m^3)
HAA-3B	GE	2.72 (2.5)[a]	0.5 (0.5)	1.5 (1.5)	8.0 E6 (6.69 E6)[b]	
HAA-3C	HEDL/SSD	2.72 (2.5)	0.5 (0.5)	1.5 (1.5)	8.0 E6 (6.69 E6)	
HAA-4	RI/ESG	2.72 (2.61)	0.5 (0.5)	1.5 (1.5)	8.0 E6 (6.69 E6)	
HAARM-3	HEDL/SSD	2.72 (2.5)	0.5 (0.5)	1.5 (1.5)	8.0 E6 (6.69 E6)	
HAARM-3	BCL	2.72 (2.5)	0.5 (0.5)	1.5 (1.5)	8.0 E6 (6.16 E6)	
HAARM-3	ORNL	2.72 (2.72)	0.5 (0.5)	1.5 (1.5)	8.0 E6 (6.16 E6)	
QUICK	BCL	2.72 (2.5)	0.5 (0.5)	1.5 (1.5)		0.68 (0.52)
QUICK	ORNL	2.72 (2.72)	0.5 (0.5)	1.5 (1.5)		0.68 (0.52)
MSPEC	BCL	2.72 (2.5)	0.5 (0.5)	1.5 (1.5)		0.68 (0.52)
MAEROS	HEDL/CSA	2.72 (2.5)	~1.5 (0.21)	H[c] (1.0)		0.68 (0.52)
CONTAIN	SNL	2.72 (2.5)	0.5 (0.5)	1.5 (1.5)		0.68 (0.52)

(a) Ex-parenthesis numbers are pretest; numbers within parenthesis are post-test.
(b) 8.0 E6 means 8.0×10^6.
(c) A histogram distribution was used.

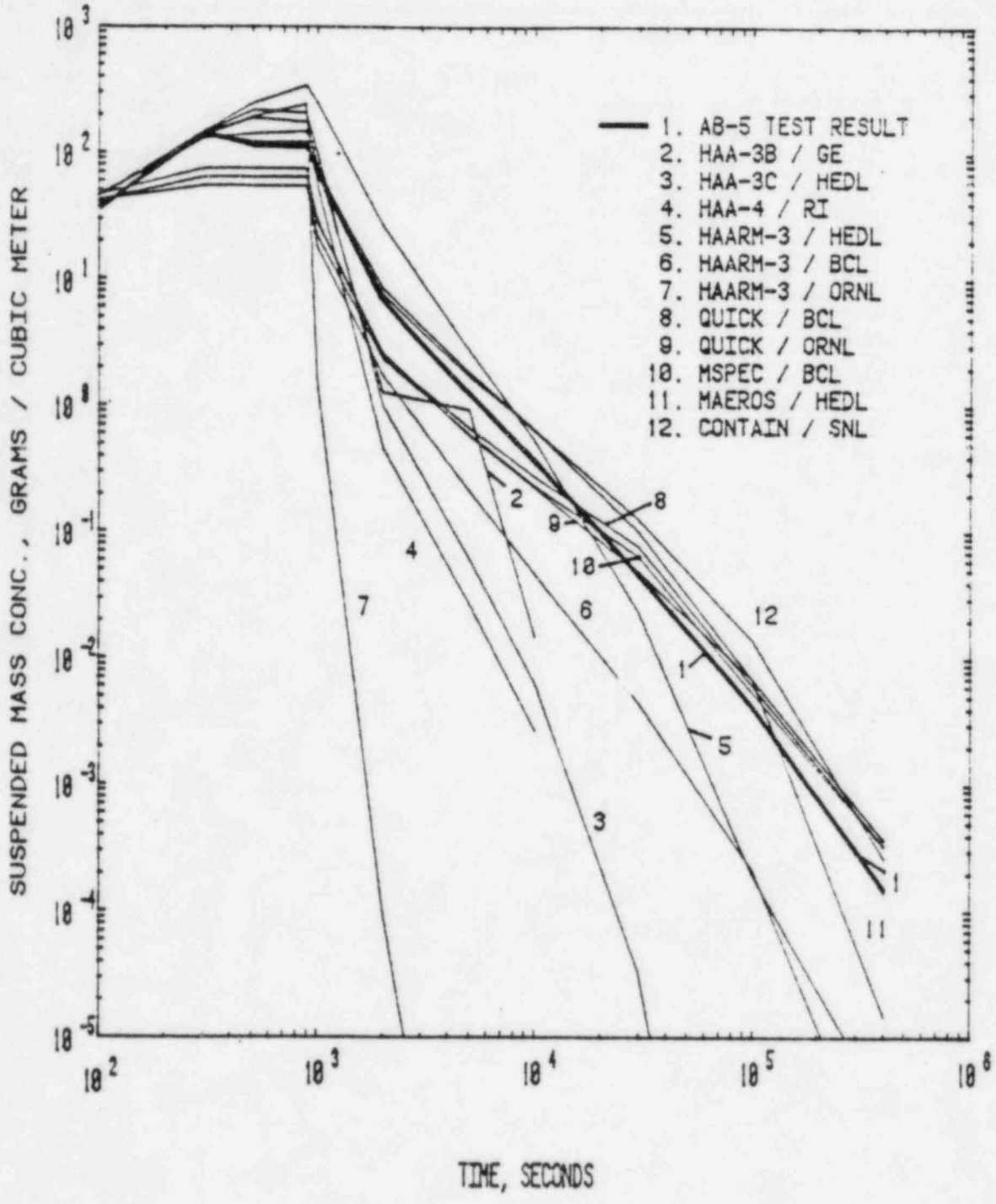

Plot of Code Predictions of Suspended Mass Concentrations for the Entire Test Period.

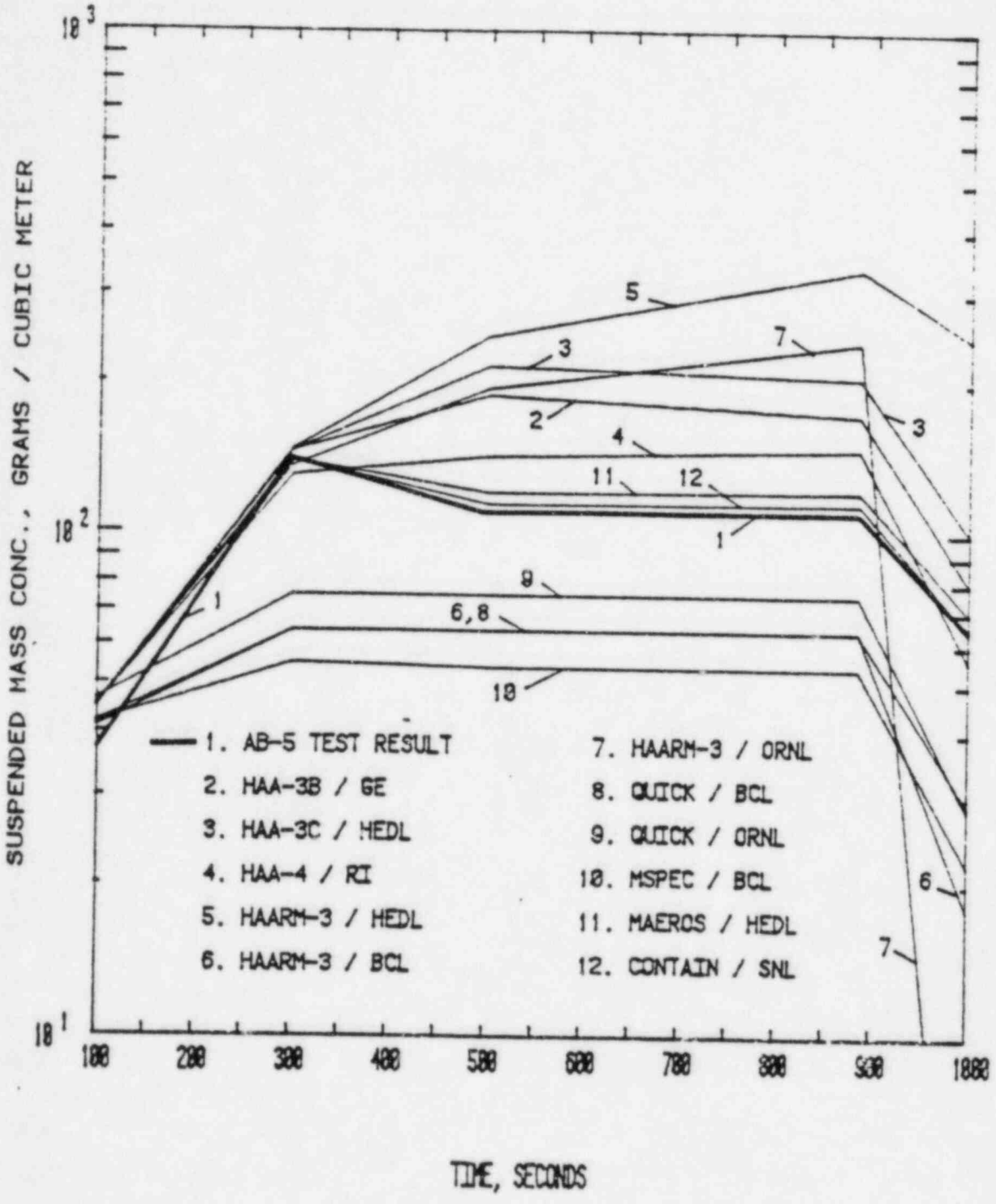

Plot of Code Predictions of Suspended Mass Concentrations During Source Period.

CODE CASES WITH CORRECT PREDICTIONS
FOR SUSPENDED MASS CONCENTRATION

Time (sec)	Code Case[a,d] 1	2	3	4	5	6	7	8	9	10	11
100	X[c]	X	X	X	X	X	X	X	X	X	X
300	X	X	X	X		X		X	X	X	X
500	X	X	X		X	X	X	X	X	X	X
885	X	X	X		X		X	X	X	X	X
1(3)[b]	X	X	X							X	X
2(3)										X	X
5(3)	X						X			X	X
1(4)				X			X	X	X	X	X
3(4)	--		--			--	X	X	X		
1(5)	--		--			--	X	X	X	X	
4(5)	--	--	--			--					X
TOTAL CORRECT	6	5	5	3	3	3	7	7	6	9	9

(a)See the curve/code identification below.
(b)Number in parenthesis is exponent of 10.
(c)An X indicates that code predicted within a factor of 2 for the indicated time.
(d)A dash indicates that no data were submitted by the code user.

CURVE/CODE IDENTIFICATION

Code Number	Code	Code Number	Code	Code Number	Code
1	HAA-3B	5	HAARM-3	9	MSPEC
2	HAA-3C	6	HAARM-3	10	MAEROS
3	HAA-4	7	QUICK	11	CONTAIN
4	HAARM-3	8	QUICK		

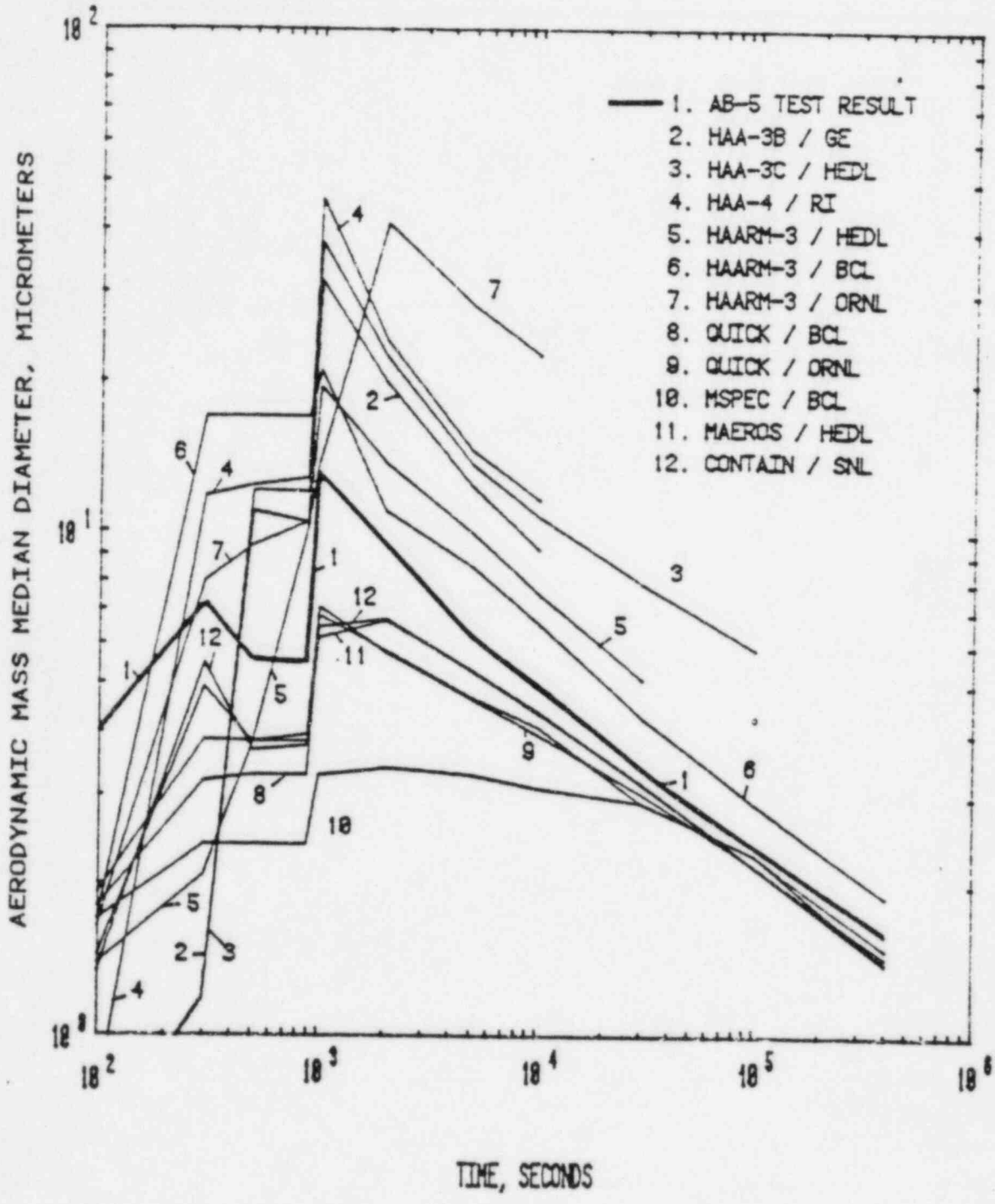

Plot of Code Predictions of Aerodynamic Mass Median Diameter.

CODE CASES WITH CORRECT PREDICTIONS
FOR AERODYNAMIC MASS MEDIAN DIAMETER

Time (sec)	Code Case[a,d] 1	2	3	4	5	6	7	8	9	10	11
100											
300						X[c]				X	X
500				X				X		X	X
885								X		X	X
1(3)[b]				X		X					
2(3)				X	X					X	X
5(3)					X		X	X		X	X
1(4)				X	X		X	X		X	X
3(4)	--		--	X	X	--	X	X	X	X	X
1(5)	--		--	--	X	--	X	X	X	X	X
4(5)	--	--	--	--	X	--	X	X	X	X	X
TOTAL CORRECT	0	0	0	5	6	1	5	7	3	9	9

(a) See the curve/code identification below.
(b) Number in parenthesis is exponent of 10.
(c) An X indicates that code predicted within a factor of 1.5 for the indicated time.
(d) A dash indicates that no data were submitted by the code user.

CURVE/CODE IDENTIFICATION

Code Number	Code	Code Number	Code	Code Number	Code
1	HAA-3B	5	HAARM-3	9	MSPEC
2	HAA-3C	6	HAARM-3	10	MAEROS
3	HAA-4	7	QUICK	11	CONTAIN
4	HAARM-3	8	QUICK		

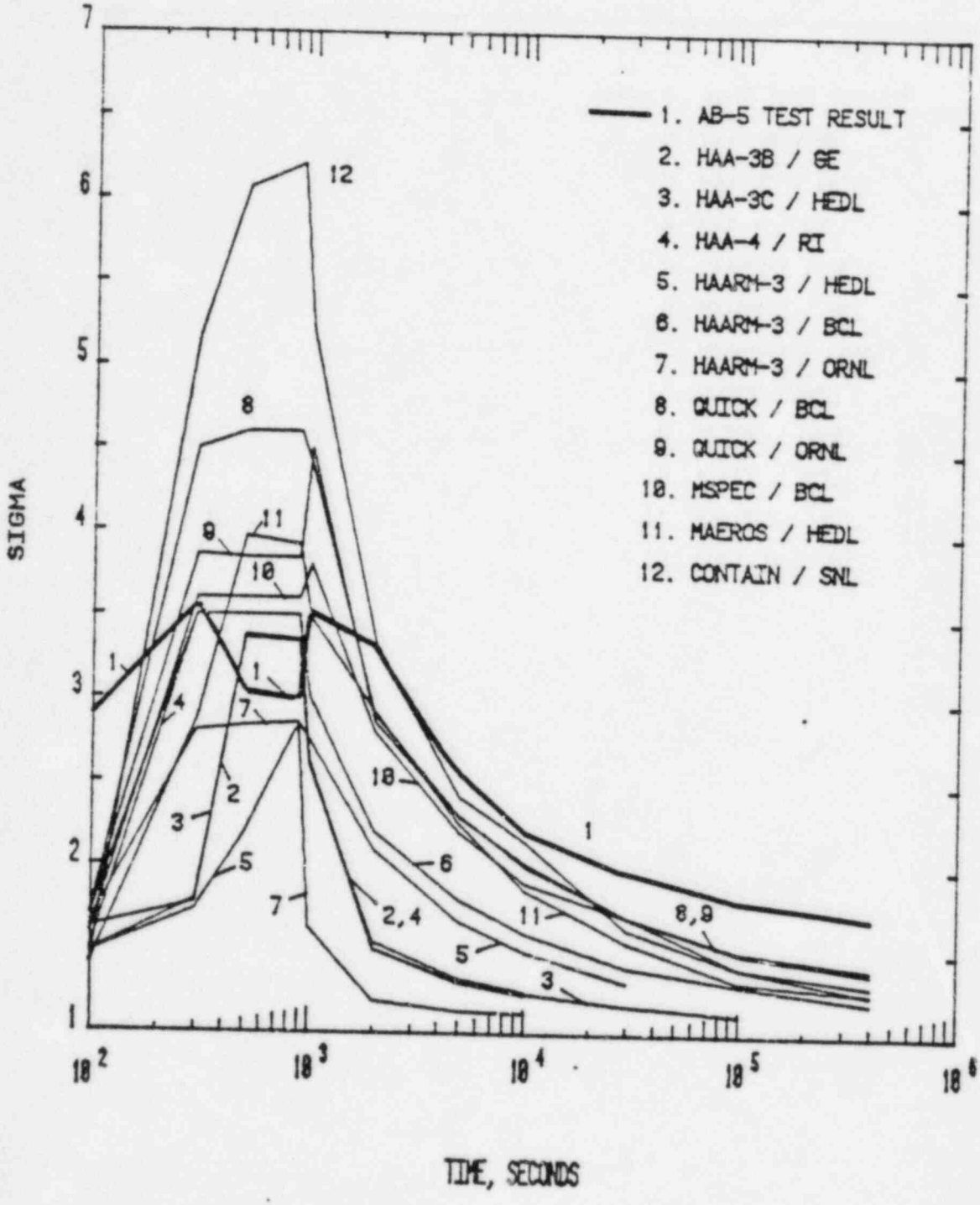

Plot of Code Predictions of Geometric Standard Deviation.

CODE CASES WITH CORRECT PREDICTIONS
FOR GEOMETRIC STANDARD DEVIATION

Time (sec)	Code Case[a,d] 1	2	3	4	5	6	7	8	9	10	11
100											
300			X		X	X	X	X	X	X	X
500	X[c]	X	X	X		X	X	X	X	X	
885	X	X	X	X	X	X	X	X	X	X	
1(3)[b]	X	X	X	X	X		X	X	X	X	X
2(3)					X		X	X	X	X	X
5(3)					X		X	X	X	X	X
1(4)				X	X		X	X	X	X	X
3(4)	--		--		X	--	X	X	X	X	X
1(5)	--		--	--	X	--	X	X	X	X	X
4(5)	--	--	--	--	X	--	X	X	X	X	X
TOTAL CORRECT	3	3	4	4	10	3	10	10	10	10	8

(a) See the curve/code identification below.
(b) Number in parenthesis is exponent of 10.
(c) An X indicates that code predicted within a factor of 1.5 for the indicated time.
(d) A dash indicates that no data were submitted by the code user.

CURVE/CODE IDENTIFICATION

Code Number	Code	Code Number	Code	Code Number	Code
1	HAA-3B	5	HAARM-3	9	MSPEC
2	HAA-3C	6	HAARM-3	10	MAEROS
3	HAA-4	7	QUICK	11	CONTAIN
4	HAARM-3	8	QUICK		

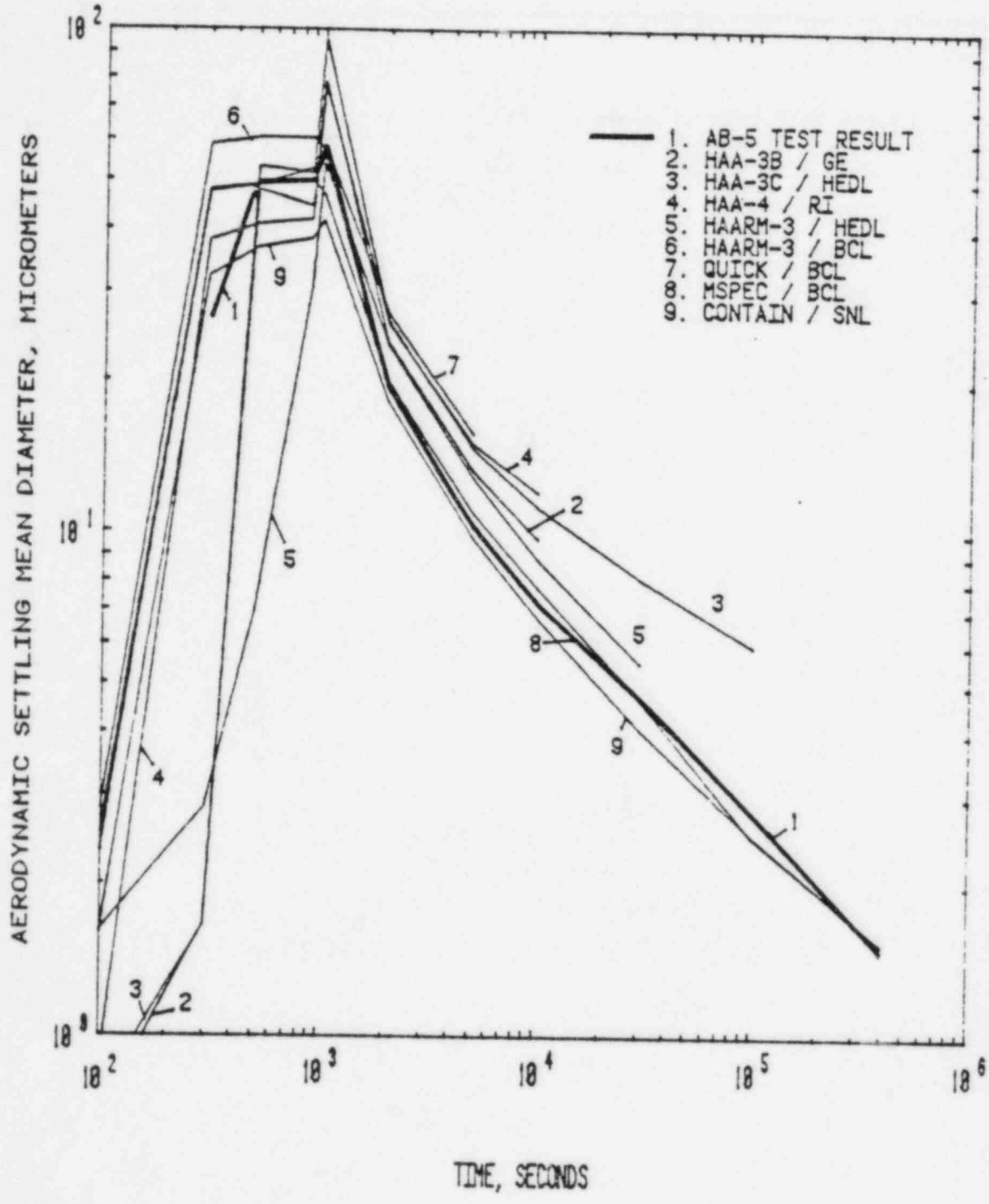

Plot of Code Predictions of Aerodynamic Settling Mean Diameter.

CODE CASES WITH CORRECT PREDICTIONS
FOR AERODYNAMIC SETTLING MEAN DIAMETER

Time (sec)	Code Case[a,e] 1	2	3	4	5	6	7	8	9	10	11
100											
300			X[c]			--		--		--	X
500	X	X	X		X	--	X	--	X	--	X
885	X	X	X		X	--	X	--	X	--	X
1(3)[b]				X	X	--	X	--	X	--	X
2(3)	X	X	X	X	X	--	X	--	X	--	X
5(3)	X	X	X	X	--	--	X	--	X	--	X
1(4)	X	X		X	--	--		--	X	--	X
3(4)	--	--	--	X	--	--		--	X	--	X
1(5)	--	--	--	--	--	--		--	X	--	X
4(5)	--	--	--	--	--	--		--	X	--	X
TOTAL CORRECT	5	5	5	5	4	(d)	5	(d)	9	(d)	10

(a) See the curve/code identification below.
(b) Number in parenthesis is exponent of 10.
(c) An X indicates that code predicted within a factor of 1.5 for the indicated time.
(d) Not reported.
(e) A dash indicates that no data were reported at that time.

CURVE/CODE IDENTIFICATION

Code Number	Code	Code Number	Code	Code Number	Code
1	HAA-3B	5	HAARM-3	9	MSPEC
2	HAA-3C	6	HAARM-3	10	MAEROS
3	HAA-4	7	QUICK	11	CONTAIN
4	HAARM-3	8	QUICK		

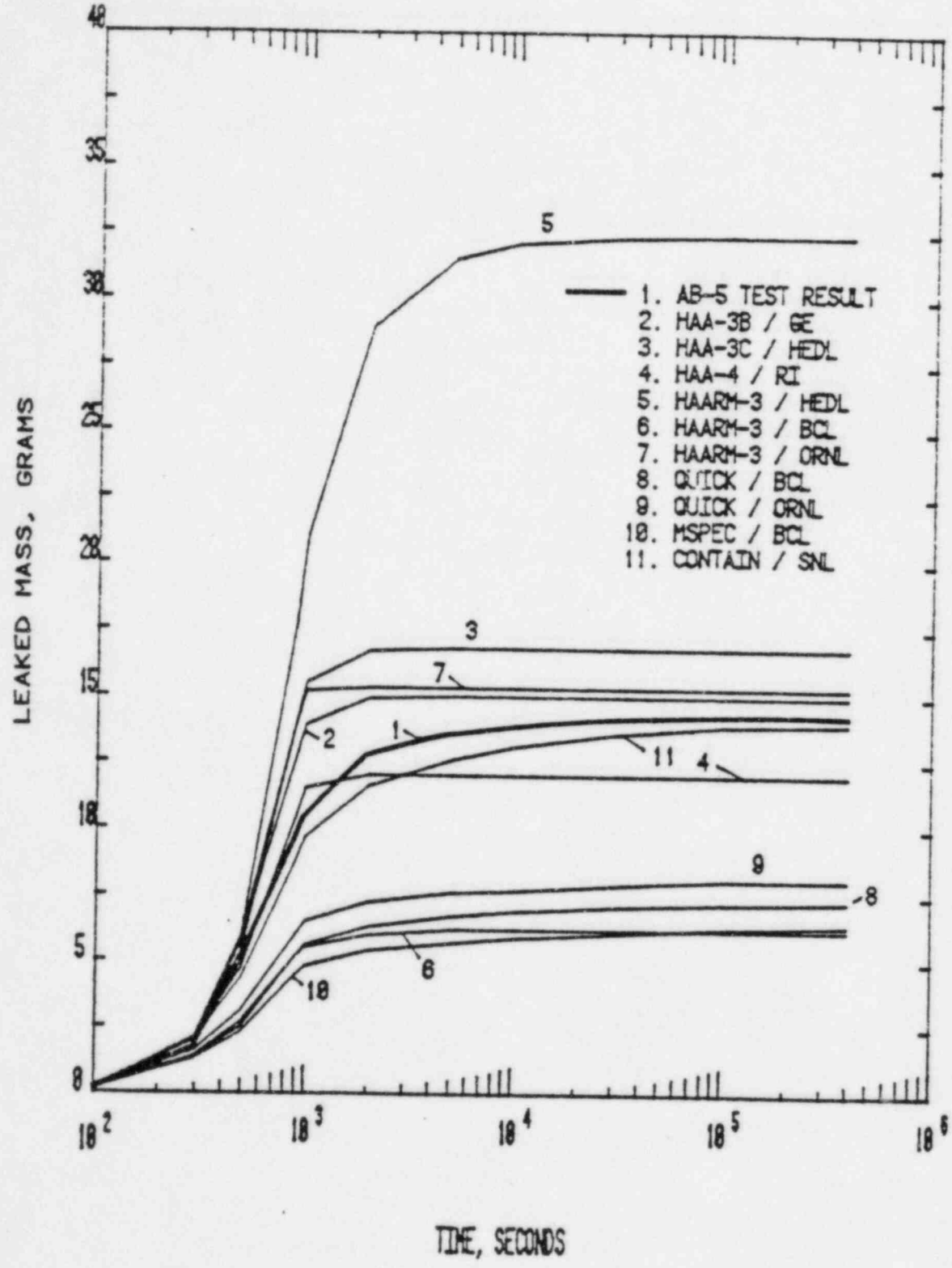

Plot of Code Predictions of Leaked Mass.

CODE CASES WITH CORRECT PREDICTIONS
FOR LEAKED MASS

Time (sec)	Code Case[a] 1	2	3	4	5	6	7	8	9	10	11
100	X[c]	X	X	X	X	X	X	X	X		X
300	X	X	X	X	X	X	X	X	X		X
500	X	X	X	X	X	X	X	X			X
885	X	X	X	X	X	X	X	X			X
1(3)[b]	X	X	X		X	X	X	X			X
2(3)	X	X	X			X	X	X			X
5(3)	X	X	X			X	X	X			X
1(4)	X	X	X			X	X	X			X
3(4)	X	X	X			X	X	X			X
1(5)	X	X	X			X	X	X			X
4(5)	X	X	X			X	X	X			X
TOTAL CORRECT	11	11	11	4	5	11	11	11	2	(d)	11

(a) See the curve/code identification below.
(b) Number in parenthesis is exponent of 10.
(c) An X indicates that code predicted within a factor of 2 for the indicated time.
(d) Not reported.

CURVE/CODE IDENTIFICATION

Code Number	Code	Code Number	Code	Code Number	Code
1	HAA-3B	5	HAARM-3	9	MSPEC
2	HAA-3C	6	HAARM-3	10	MAEROS
3	HAA-4	7	QUICK	11	CONTAIN
4	HAARM-3	8	QUICK		

SUMMARY OF LEAKED MASS PREDICTIONS

Code	User	Ratio: Code to Test
HAA-3B	GE	1.05
HAA-3C	HEDL/SSD	1.17
HAA-4	RI/ESG	0.84
HAARM-3	HEDL/SSD	2.26
HAARM-3	BCL	0.43
HAARM-3	ORNL	1.07
QUICK	BCL	0.51
QUICK	ORNL	0.56
MSPEC	BCL	0.45
MAEROS	HEDL/CSA	--
CONTAIN	SNL	0.98
AVERAGE		0.937

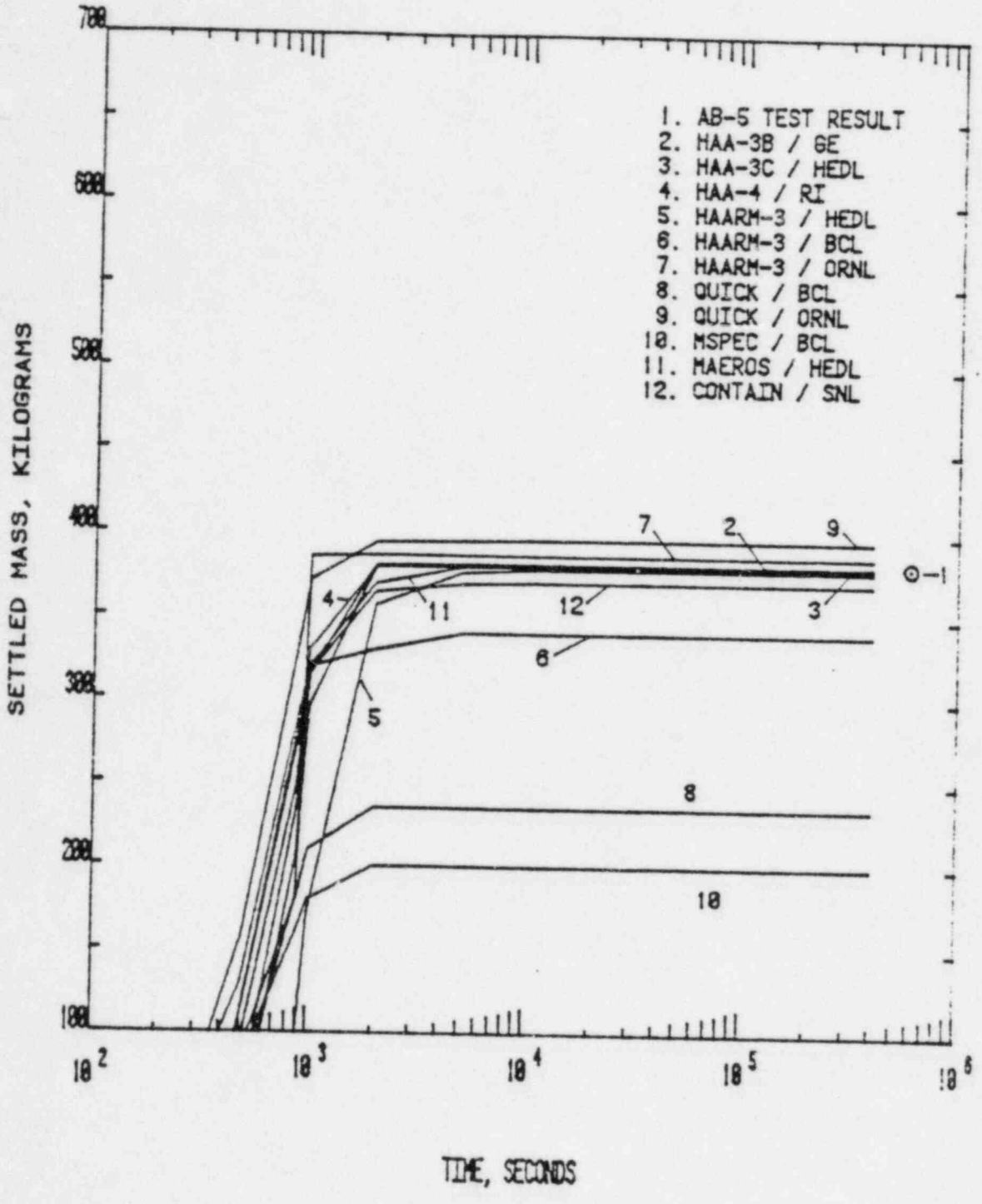

Plot of Code Predictions of Settled Mass.

CODE CASES WITH CORRECT PREDICTIONS
FOR SETTLED MASS

Time (sec)	Code Case[a] 1	2	3	4	5	6	7	8	9	10	11
1(4)[b,c]	X[d]	X	X	X	X			X		X	X
3(4)	X	X	X	X	X	X		X		X	X
1(5)	X	X	X	X	X	X		X		X	X
4(5)	X	X	X	X	X	X		X		X	X
TOTAL CORRECT	4	4	4	4	4	4	0	4	0	4	4

(a) See the curve/code identification below.
(b) Number in parenthesis is exponent of 10.
(c) Experimental result not available at $t < 10^4$.
(d) An X indicates that code predicted within ±15% for the indicated time.

CURVE/CODE IDENTIFICATION

Code Number	Code	Code Number	Code	Code Number	Code
1	HAA-3B	5	HAARM-3	9	MSPEC
2	HAA-3C	6	HAARM-3	10	MAEROS
3	HAA-4	7	QUICK	11	CONTAIN
4	HAARM-3	8	QUICK		

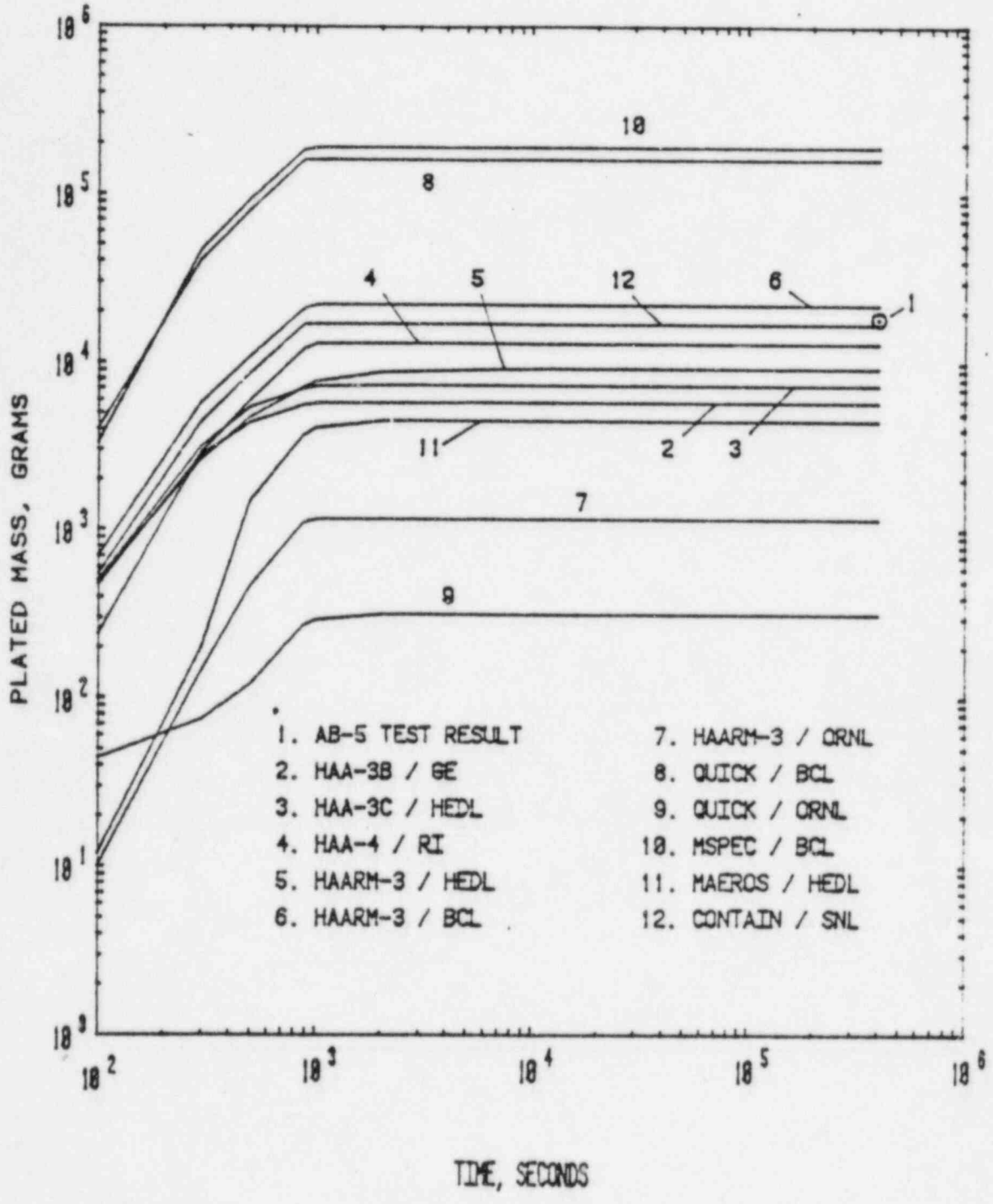

Plot of Code Predictions of Plated Mass.

CODE CASES WITH CORRECT PREDICTIONS
FOR PLATED MASS(b)

Code Case(a)	Predicted Plated Mass Within Factor of 2	
	YES	NO
1		X
2		X
3	X	
4	X	
5	X	
6		X
7		X
8		X
9		X
10		X
11	X	

(a) See the curve/code identification below.

(b)For end-of-test conditions.

CURVE/CODE IDENTIFICATION

Code Number	Code	Code Number	Code	Code Number	Code
1	HAA-3B	5	HAARM-3	9	MSPEC
2	HAA-3C	6	HAARM-3	10	MAEROS
3	HAA-4	7	QUICK	11	CONTAIN
4	HAARM-3	8	QUICK		

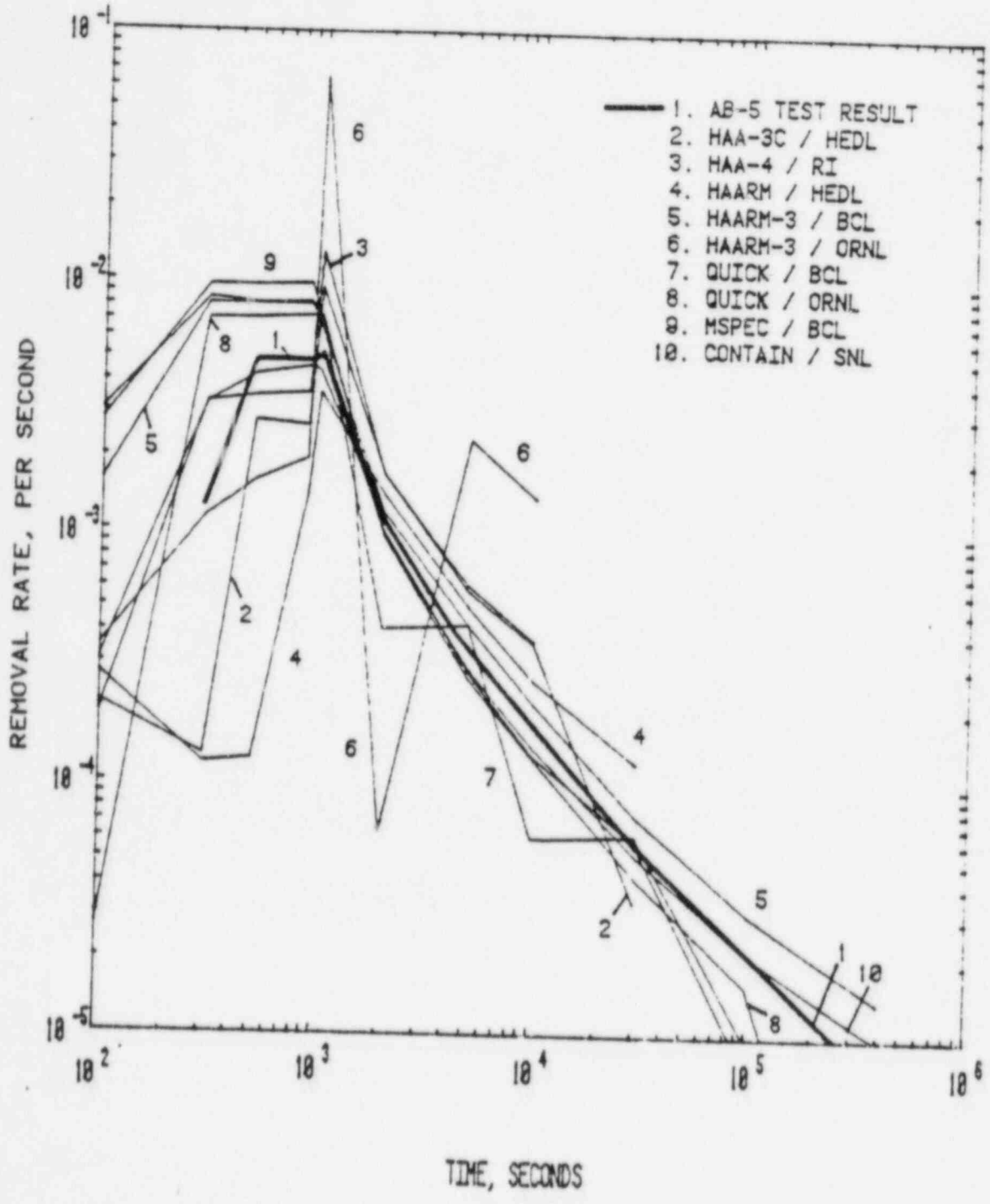

Plot of Code Predictions of Overall Removal Rate.

CODE CASES WITH CORRECT PREDICTIONS FOR REMOVAL RATE

Time (sec)	Code Case(a,e) 1	2	3	4	5	6	7	8	9	10	11
100											
300						X					
500		X(c)	X		X		X	X	X		X
885		X	X		X		X	X	X		X
1(3)(b)				X	X		X	X	X		X
2(3)		X	X	X	X			X	X		X
5(3)		X	X	X	X		X	X	X		X
1(4)				X	X			X	X		X
3(4)		X	--		X	--	X	X	X		X
1(5)		--	--	--	X	--		X			X
4(5)		--	--	--	X	--	X		X		X
TOTAL CORRECT	(d)	5	4	4	9	1	6	8	8	(d)	9

(a) See the curve/code identification below.
(b) Number in parenthesis is exponent of 10.
(c) An X indicates that code predicted within a factor of 2 for the indicated time.
(d) Not reported.
(e) A dash indicates that data on removal rate were not reported at this time.

CURVE/CODE IDENTIFICATION

Code Number	Code	Code Number	Code	Code Number	Code
1	HAA-3B	5	HAARM-3	9	MSPEC
2	HAA-3C	6	HAARM-3	10	MAEROS
3	HAA-4	7	QUICK	11	CONTAIN
4	HAARM-3	8	QUICK		

COMPARISON OF PRETEST AND BLIND POST-TEST PREDICTIONS

Time (s)	Geometric Mean of All Codes, Ratio of Post-Test/Pretest							
	Susp. Conc.	AMMD	σ_g	ASMD	M_L	M_S	M_P	R
1(2)	0.67	0.77	0.81	1.16	0.58	0.49	0.44	0.96
3(2)	0.76	1.00	1.00	2.08	0.70	0.69	0.62	0.96
5(2)	0.75	0.93	1.02	1.45	0.72	0.84	0.56	0.99
8.85(2)	0.73	0.93	1.09	1.43	0.70	0.80	0.64	1.06
1(3)	0.64	0.87	1.02	1.19	0.72	0.86	0.62	1.89
2(3)	0.68	1.11	1.03	0.92	0.69	0.55	0.61	0.70
5(3)	0.70	1.11	1.03	0.97	0.68	0.77	0.61	1.33
1(4)	0.54	1.24	1.00	0.89	0.68	0.77	0.61	1.58
3(4)	0.75	0.93	1.05	1.07	0.68	0.77	0.61	0.95
1(5)	0.80	0.94	1.03	1.00	0.68	0.77	0.61	0.95
4(5)	1.41	0.89	1.06	1.60	0.68	0.77	0.61	1.28

COMPARISON OF SUSPENDED CONCENTRATIONS PREDICTED
BY LOG-NORMAL AND DISCRETE CODES

Time (s)	Geometric Mean Concentration (g/m^3)		Measured Concentration (g/cm^3)
	Log-Normal Codes	Discrete Codes	
100	4.4 (1)	4.4 (1)	3.7 (1)
300	1.1 (2)	8.7 (1)	1.4 (2)
500	1.4 (2)	8.1 (1)	1.1 (2)
885	1.4 (2)	8.2 (1)	1.1 (2)
1000	6.0 (1)	3.8 (1)	6.5 (1)
2000	9.0 (-1)	3.9 (0)	6.8 (0)
5000	2.5 (-1)	9.3 (-1)	1.2 (0)
10000	2.7 (-2)	3.5 (-1)	3.8 (-1)
30000	2.1 (-3)	7.9 (-2)	4.7 (-2)

COMPARISON OF PARTICLE SIZE PARAMETER
PREDICTED BY LOG-NORMAL AND DISCRETE CODES

Time	Geometric Mean of AMMD (μm)			Geometric Mean σ_g			Geometric Mean of Aerodynamic Settling Mean Diameter (μm)		
(sec)	Log-N	Discrete	Test	Log-N	Discrete	Test	Log-N	Discrete	Test
100	1.10	1.64	4.0	1.58	1.57	2.9	1.34	2.02	--
300	9.16	3.97	7.2	2.66	4.00	3.55	20.6	42.7	26.
500	13.0	3.41	5.6	3.26	4.42	3.05	42.0	45.0	50.
885	14.2	3.46	5.5	3.36	4.43	3.00	45.9	47.1	50.
1000	30.5	5.97	13.0	2.78	4.28	3.50	72.8	52.6	47.
2000	17.2	5.67	9.4	1.85	2.96	3.3	23.9	21.7	20.
5000	11.4	4.65	6.2	1.54	2.29	2.55	14.0	11.9	11.
10000	8.81	3.99	5.0	1.40	1.99	2.2	10.4	7.0	7.8
30000	5.47	3.03	3.4	1.27	1.42	1.97	6.8	4.4	4.7

A Comparison of Aerosol Behavior Codes

J. A. Gieseke
Battelle Columbus Laboratories

A COMPARISON OF AEROSOL BEHAVIOR CODES

by

J. A. Gieseke
Battelle Columbus Laboratories

There are a number of mechanistic aerosol behavior codes developed to evaluate the transport, deposition, and leakage of fission products in reactor containments. Most of the codes have evolved from models designed for analyses of aerosols in LMFBR systems and therefore include to varying degrees, mechanisms added to extend their applicability to LWR conditions. Among the codes available for containment analyses are several which were developed for fission product behavior in primary systems. These are also applicable to containment conditions through their ability to analyze aerosol behavior in general and in some cases have been used for containment analyses. The CORRAL code, even though historically important, has not been included in the comparison since it is largely empirical.

The major technical features or aerosol behavior mechanisms included in all of the codes are listed in the attached table where the inclusion or exclusion of each mechanism in each of the various codes is noted. A brief discussion of the major features and differences among the codes is provided to supplement the tabular information.

There are two major classes of codes, those developed for the containment and those developed for the primary system (RAFT, RETAIN, TRAP-MELT 2). The RETAIN code has been extended for use in the containment and TRAP-MELT C is an adaptation of the TRAP-MELT 2 code for containment conditions. Primary system codes include fission product vapor interactions with aerosols and surfaces and do not consider water condensation, although the TRAP-MELT C code is an exception in this regard. The containment codes are focused on aerosol behavior under containment conditions with steam condensation on aerosols and surfaces. The MATADOR code, which is a fairly mechanistic code for risk assessment and is intended to be a replacement for CORRAL, treats noble gases and fission product vapor (assumed to be I_2) in addition to aerosols.

A significant difference in representation of the aerosol size distribution exists among the codes with the ABC-3C, HAA-4A, HAARM-3, MATADOR, and RETAIN codes assuming a log-normal distribution. The log-normal distribution has been shown, by comparison with experiments,

to overestimate aerosol depletion rates, and the codes using a discretized or sectionalized size range show much better agreement with experiments and are therefore much preferred.

Related to the size representation is the question of aerosol composition as a function of size. Only the QUICKM and MAEROS codes compute composition by size range, with other codes following only water/solid aerosol ratios with size (NAUA-4, TRAP-MELT C) or assuming equal composition for all particle sizes. It should be noted that the QUICKM code is the only code that tracks aerosol material density and shape factors as a function of size (composition). The theoretical basis for size dependent composition is quite appealing and significant effects on airborne materials are computed for some circumstances; however, there is not yet a definitive experimental basis for supporting the code predictions. Experimental work in this area is progressing and the second multicomponent ABCOVE experiment was matched fairly well in aerosol composition by the QUICKM code. However, the use of codes treating size dependent composition should proceed cautiously until considerably more experimental data are available.

There are some situations in the progression of accidents where homogeneous nucleation of aerosols may be important. The first situation would involve rapid steam injection into the containment with low aerosol concentrations such that the gas becomes supersaturated with water vapor and homogeneous nucleation would occur in parallel with condensation on pre-existing particles. The NAUA-4 Mod code permits homogeneous nucleation of water to take place under these conditions. A second situation could exist for BWR cases in which decay heating in the containment is considered, the drywell volume may reach temperatures at which many fission products are vapors and the timing is such that previously existing aerosol species have been swept from the volume. As fission product vapors move from the drywell volume or as the drywell temperature drops, homogeneous nucleation is expected to occur. Similar situations can exist within the primary system. Another situation can exist where effects of hydrogen burning may be such to produce vaporized fission products while there is a low non-volatile aerosol component airborne. Again homogeneous nucleation may be important as cooling occurs. Only the RAFT code includes homogeneous nucleation. However, it is unlikely that truly homogeneous nucleation can occur in the high ion concentrations expected in a radiation environment so the issue and inclusion of homogeneous nucleation is subject to further evaluation.

In general, the aerosol behavior codes using discretized size distributions have been found to predict experimental results with good accuracy (to within a factor of 3 for airborne mass concentrations) in blind predictions. A summary of predictions with some of the codes compared with ABCOVE experiment AB-5 are shown in the attached figure. The agreement between experiment and predictions for codes using a discretized size distribution is quite encouraging and suggests that major processes are being modeled successfully.

AEROSOL BEHAVIOR CODES AND MECHANISMS

	ABC-3C (Japan)	AEROSIM (UK)	AEROSOL (France)	CONTAIN/MAEROS (SNL)	HAA-4A (AI)	HAARM-3 (BCL)	MATADOR (BCL)	NAUA-4 Mod (FRG/BCL)	PARDISEKO-3 (FRG)	QUICK (BCL)	QUICKM (BCL)	RAFT (ANL)	RETAIN (IDCOR)	TRAP-MELT 2 (BCL)	TRAP-MELT C (BCL)	ZONE (BCL)
Agglomeration																
Brownian	X	X	X	X	X	X	X	X	X	X	X	X	X	X	X	X
Gravitational	X	X	X	X	X	X	X	X	X	X	X	X	X	X	X	X
Turbulent	X	X	X	X	X	X	X	X	X	X	X	X	X	X	X	X
Inertial	-	-	-	-	-	-	-	-	-	-	-	-	X	-	-	-
Removal																
Diff, Lam	a	a	a	a	a	a	a	a	a	a	a	X	X	X	X	a
Diff, Turb	-	-	-	-	-	-	-	-	-	-	-	X	X	X	X	a
Settling	X	X	X	X	X	X	X	X	X	X	X	X	X	X	X	X
Stefan flow	-	X	-	X	-	-	X	X	-	-	X	-	-	-	X	-
Thermophoresis	X	X	X	X	X	X	X	-	-	X	X	X	X	X	X	X
Inertial impaction	-	-	-	-	-	-	-	-	-	-	-	-	X	-	-	-
Leakage (flow)	X	X	X	X	X	X	X	X	X	X	X	X	X	X	X	X
Sprays	-	-	-	X	-	-	X	X	-	-	-	-	-	-	-	-
Ice beds	-	-	-	-	-	-	-	X	-	-	-	-	-	-	-	-
Resuspension	-	-	-	-	-	-	-	-	-	-	-	b	c	b	b	-
Interactions																
Steam cond on aerosols	-	X	X	X	-	-	-	X	-	-	X	-	-	-	X	-
Nucleation, fp	-	-	-	-	-	-	-	-	-	-	-	X	-	-	-	-
Nucleation, steam	-	-	-	-	-	-	-	X	-	-	-	-	-	-	-	-
Discretized sizes	-	X	X	X	-	-	d	X	X	X	X	X	-	X	X	X
Aerosol composition with size	-	-	-	X	-	-	-	e	-	-	X	X	-	-	e	-
Multi-compartment	X	-	X	X	-	-	-	-	-	-	-	X	f	X	X	-
F.P. Vapors Included	-	-	-	-	-	-	g	-	-	-	-	X	X	X	X	-

(a) Not specific, uses input boundary layer.
(b) Resuspension by deposit vaporization.
(c) Resuspension by deposit vaporization plus as input for aerosols.
(d) Log-normal for agglomeration and gravitational settling only, discrete otherwise.
(e) Water vapor/aerosol ratio only.
(f) Sequential volumes only.
(g) Vapor (as I_2) and noble gases.

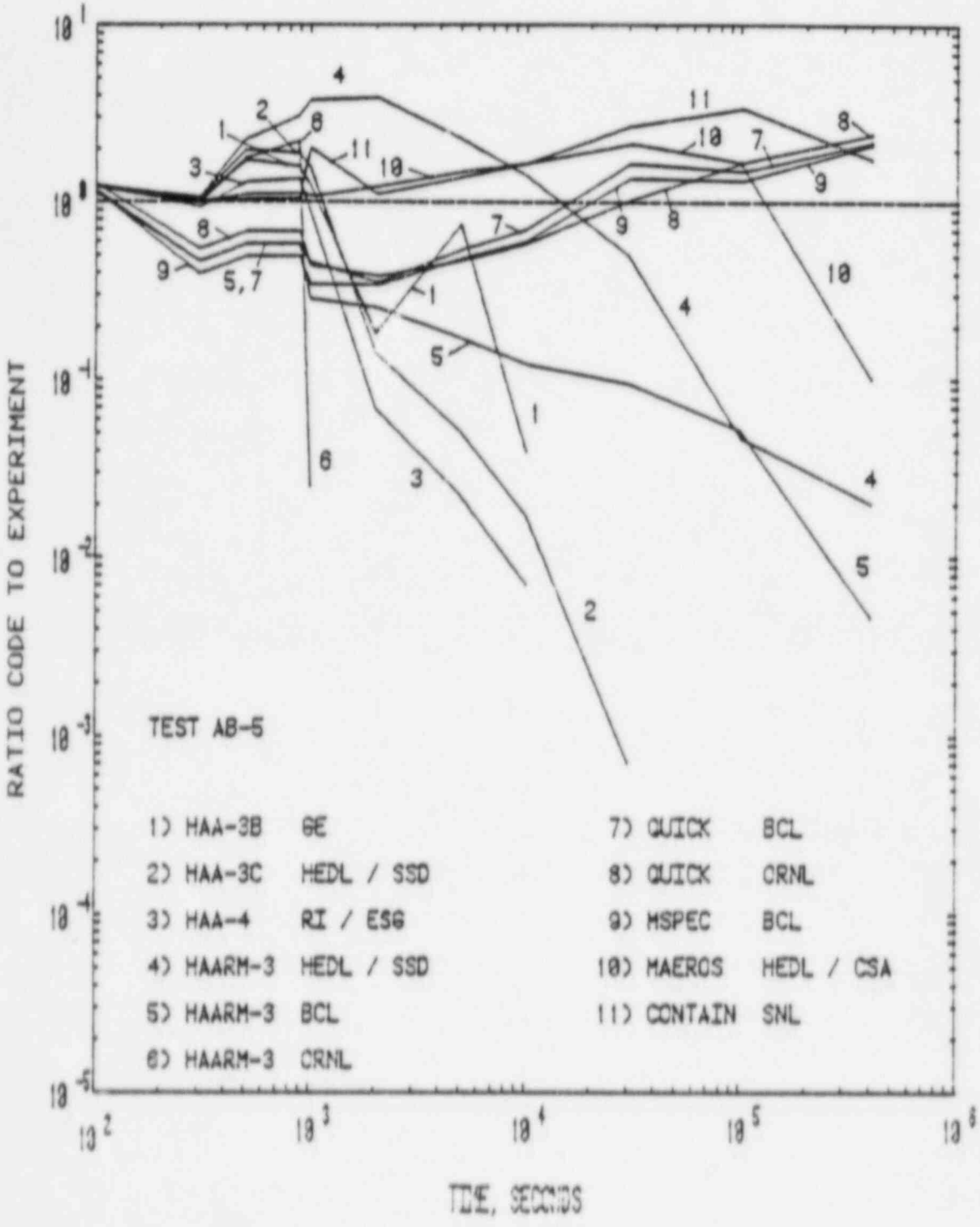

Ratios of Code Prediction to Experiment for Suspended Mass Concentration -- Test AB5.